Theory of electromigration failure in polycrystalline metal films

Kang Wu and R. Mark Bradley
Department of Physics, Colorado State University, Fort Collins, Colorado 80523
(Received 13 July 1994)

We introduce a dynamic fuse model for the damage done to a current-carrying polycrystalline metal thin film by electromigration. We determine the exact scaling behavior of the crack tip velocity for a single crack oriented perpendicularly to the direction of the ambient current. A Lifshitz-type theory works well only when the initial density of defects (p) is small. For all p, the mean failure time is to an excellent approximation proportional to the average length of the shortest path across the film in a certain metric. This conclusion is supported by our simulations and by analytical work based on a variational formulation of our problem. Using the shortest-path approximation, we show that the mean failure time tends to zero as $(p_c - p)^{4/3}$ as the percolation threshold $p = p_c$ is approached. We also use the shortest-path approximation to account for experimental results on the lifetime of long polycrystalline metal wires of varying lengths and widths.

I. INTRODUCTION

When a high current density passes through a thin metal film, collisions between the conduction electrons and the metal ions lead to drifting of the ions. This process is known as electromigration.[1–3] If there is a divergence in the flux of ions at a point, a void or hillock forms.[4] Voids grow and overlap until conduction ceases and electrical failure is complete.

As integrated circuits become progressively more complex, the individual components must become increasingly more reliable if the reliability of the whole is to be acceptable. However, due to the continuing miniaturization of very large scale integrated circuits, the metallic thin films used as conductors are subject to increasingly high current densities. Under these conditions, electromigration can lead to the electrical failure of interconnects in relatively short times, thereby reducing the circuit lifetime to an unacceptable level.[5] It is therefore of great technological importance to understand and control electromigration failure in thin films.

Electromigration in crystalline metals proceeds by lattice diffusion driven by the "electron wind," and is now relatively well understood.[1–3] In polycrystalline metal thin films at low temperatures, however, ionic transport proceeds mainly by grain boundary diffusion.[4] Typically, the temperature in these films is to a good approximation uniform, since they are in good thermal contact with the substrate. In these circumstances, divergences in the mass flow—and hence the formation of voids or hillocks—occur at three different types of inhomogeneities. A nonzero divergence will occur at a bend in a grain boundary, since the grain-boundary mobility depends on the degree of misorientation at the boundary. Similarly, mass flow divergences occur at grain-boundary triple points. Finally, an abrupt change in grain size between one region of the conductor and another will cause a flux divergence.

The grain structure determines the lifetime of a particular film, and its variation from sample to sample results in a distribution of lifetimes. It has been found experimentally[4] that the time t_{50} required for 50% of a large collection of films to fail obeys the empirical relation

$$t_{50} = A j^{-n} \exp\left[\frac{\Delta E}{k_B T}\right], \qquad (1.1)$$

where j is the current density and T is the temperature. The parameters A, n, and ΔE are adjusted to fit the data. The constant A is usually only weakly temperature dependent. The exponent n may be taken to be 1 for low current densities, but for larger j's higher values of n are needed, since Joule heating becomes significant in this regime. Finally, to a good approximation ΔE is equal to the activation energy for grain-boundary diffusion.

The first step in developing a theory of electromigration damage in polycrystalline metal films has been to study damage at a single grain boundary. The two topics that have received the most attention are the effect of electromigration on grain-boundary grooving in a bicrystal geometry[6–10] and void formation at a grain-boundary triple point.[7]

These studies concern the formation and growth of a void or hillock at a single crystalline defect. In a real polycrystalline film there are many defects that may contribute to electrical failure, and failure occurs only after the growth and coalescence of many different voids. Early attempts to deal with multiple defects were based on classical nucleation theory.[7,11] This approach has recently been revived by Rodbell, Rodriguez, and Ficalora,[12] who assume that circular voids nucleate and then grow with constant velocity, preserving their circular shape.

The approach of Rodbell *et al.* is open to a number of criticisms. Their work is purely phenomenological—neither the nucleation rates nor the void growth velocities were calculated. More importantly, whenever a void is formed in a film, the current is crowded on either side of the void. The increased current density in these re-

0163-1829/94/50(17)/12468(21)/$06.00 ©1994 The American Physical Society

gions leads to an increased rate of electromigration, so the void will become elongated in a direction normal to the ambient current. Thus, the *ad hoc* assumption of circular voids that preserve their shape cannot be correct. Experiments have in fact revealed that the void structure is much more complex and that this assumption is a poor approximation.[13,14] The theory of Rodbell *et al.* has also been criticized on different grounds by Patrinos, Vankar, and Schwarz.[15]

Failure of thin polycrystalline metal wires was studied by Monte Carlo simulation by Attardo, Rutledge, and Jack.[16] In their model, the conductor was taken to be made up of a series of short sections with different lengths, each one grain across. The length of the sections was randomly chosen according to the grain size distribution. Normal to the length of the conductor each section was made up of randomly selected grains. The atomic transport within a particular grain boundary was taken to depend on the degree of misorientation and on the angle between the current and the grain boundary. Finally, the electrical current was assumed to be uniform throughout the conductor. The time-to-failure for the wire is then inversely proportional to the maximum flux divergence between two consecutive sections. The model of Attardo, Rutledge, and Jack has been applied to very thin wires with a "bamboo" grain structure by Schoen.[17]

The *ad hoc* assumptions made by Attardo, Rutledge, and Jack on the grain structure of the conductor limit the applicability of their study. Recently, Huntington *et al.*[18] have improved on the approach of Attardo, Rutledge, and Jack by employing a more realistic grain structure in their simulations, and by taking stress-induced grain boundary motion into account. The models of Attardo, Rutledge, and Jack and Huntington *et al.* both suffer from a serious failing, however: Current crowding is entirely neglected. Clearly, as a real wire nears failure, current crowding becomes increasingly significant.

Current crowding was taken into account in a crude fashion in the analytical work of Sigsbee.[19] Sigsbee assumed that line failure occurs by the propagation of a single crack across the wire. The possibility of multiple cracks was ignored, as was the fact that the crack tip may split, leading to branching of the crack. Indeed, highly ramified, irregular void structures have been observed in polycrystalline Al films.[14]

Perhaps the most realistic simulations of electromigration carried out to date are those of Marcoux *et al.*[20] These workers explicitly took current crowding into account, and made realistic assumptions on the grain-boundary structure. Moreover, they made no *ad hoc* assumptions on the shape of the voids. Similar approaches were used by Kirchheim and Kaeber[21] and Smy, Winterton, and Brett.[22]

It has been known for some time that defects are crucial in determining the electrical and mechanical strength of materials. Recently, the ideas of percolation theory have been applied to the problem of failure of disordered materials, leading to important new progress in the field.[23–47] The simplest model that has been studied is the random fuse network.[23–27] In this model, each bond of a square lattice is occupied with a fuse with probability p and a perfect insulator with probability $1-p$. Each fuse has a resistance of 1 Ω up to its load limit of 1 V. At higher voltages, the fuse burns out and becomes an insulator. The failure process is irreversible: Once the fuse has blown, its resistance remains infinite even if the voltage across it later drops below 1 V.

Initially a very small voltage is applied across the random fuse network, and all the fuses are in their Ohmic state. We assume that $p \geq p_c$ so that conduction occurs. As the voltage is increased, a fuse first blows at some voltage V_1. Further increases in voltage lead to additional failures, and at a voltage $V_b \geq V_1$ conduction ceases and electrical failure is complete.

The electrical failure of the random fuse network is an example of a breakdown process in a random medium. Other problems in this class include dielectric breakdown in metal-loaded dielectrics,[24,27–34] the onset of superconductivity in granular superconductors,[35–39] and the fracture of brittle materials.[40–47] In each case, the basic elements of the random network undergo an irreversible change when an externally applied voltage (or stress) passes through a critical value.

Electromigration-induced damage in a polycrystalline metal film is an irreversible process, since the damage cannot be repaired simply by reversing the current. In this paper, we will develop and study a breakdown model for the damage done to a polycrystalline metal thin film by electromigration. Current crowding next to growing voids is explicitly taken into account in our model. Moreover, no *ad hoc* assumptions about void shape are made.

Our model was inspired by the random fuse model, but is fundamentally different from it, since our model is truly kinetic, while the random fuse model is not. A kinetic breakdown model has already been studied by Sornette and Vanneste.[48,49] The model of Sornette and Vanneste reduces to ours in a certain limit, but their model was introduced to describe failure of random fuse networks that burn out due to Joule heating rather than electromigration damage.

Our model is similar in spirit to that of Marcoux *et al.*[20] In both models, current crowding is taken into account and no *ad hoc* assumptions about void shape are made. However, we have chosen to concentrate on the approach to the thermodynamic limit, since this is where we expect universal behavior that is independent of the model details. Accordingly, we employ a coarse-grained description of the film in which the lower cutoff length is large compared to the grain size. In contrast, a lattice spacing smaller than the mean grain size was adopted by Marcoux *et al.* Although their model is arguably more realistic than ours, Marcoux *et al.* were only able to perform simulations. We are able to make considerable progress on our model analytically, in part because it is simpler.

The paper is organized as follows: In the following section, we introduce and motivate our model. In Sec. III, we study the growth of a single crack in a film. Two theories for the failure time of a film in which many defects are present at $t=0$ are developed in Sec. IV. We

describe the results of our Monte Carlo simulations of electromigration damage to films with multiple defects in Sec. V. These simulations provide tests of the theories developed in Sec. IV. The failure of long, narrow wires is studied in Sec. VI, and the predictions of the theory are compared with experiment. Section VII contains our conclusions.

II. THE MODEL

We begin by developing our model of electromigration failure of thin polycrystalline metal films. An atomistic molecular dynamics approach is clearly impractical because of the prohibitively large computing time needed. In lieu of this, we shall carry out a Monte Carlo study of a semimacroscopic model. We will use a coarse-grained description in which the small-scale structure is averaged over and the continuous metal film is replaced by a discrete lattice of wires. The grid spacing in our lattice is taken to be large compared to the mean grain size but small relative to the film as a whole. This approach will simplify the calculations enormously without altering the nature of large-scale phenomena occurring in the system.

As discussed in the Introduction, the lifetime of a polycrystalline metal thin film is greatly influenced by the structural disorder present. We must therefore take into account the random variations in the resistances of the wires in our coarse-grained description of the system. In principle, the probability distribution of the resistances could be computed from a detailed knowledge of the grain structure. The statistical distribution of grain sizes and orientations depends strongly on both the material and the method of preparation, however. Because the type of disorder present is usually very complex and poorly characterized, as a first step we will study electromigration failure in a system with a particularly simple type of disorder. Thus, to be specific, we consider a regular square grid of points. Each nearest-neighbor set of points in the grid is joined by either a conducting wire with resistance R (with probability $1-p$) or by an insulator (with probability p). This simple percolative disorder is meant to mimic the disordered crystal structure in a real polycrystalline metal film.

We must now take into account the fact that when a current I passes through a particular wire, electromigration occurs and electrical failure eventually takes place. In so doing, we cannot neglect the variation of I with time, since failures elsewhere in the system may lead to current redistribution.

Let us suppose that a certain mass m_c must leave the wire before failure occurs. The mass flux j_m within the wire is

$$j_m = \frac{N_a D}{k_B T} Z^* e E \ , \tag{2.1}$$

where N_a is the atomic density, D is the diffusivity, $Z^* e$ is the effective charge, and E is the electric field strength.[4] The total mass flow out of the wire r is therefore proportional to the magnitude of the current I:

$$r = \kappa(T)|I| \ . \tag{2.2}$$

The temperature-dependent constant of proportionality is

$$\kappa(T) \equiv \frac{N_a D}{k_B T} Z^* e \rho \ , \tag{2.3}$$

where ρ is the resistivity.

In microelectronics applications, the substrate is silicon, and Si has a high thermal conductivity. The Joule heat generated in the wire is therefore rapidly conducted away by the substrate. Accordingly, the temperature of the wire T will be very nearly equal to the temperature of the substrate T_0 unless the current through the wire is very large. Thus, we may ignore the effect of Joule heating and take T and T_0 to be equal.

We now see that the lifetime of the wire t_f is given by

$$\int_0^{t_f} |I(t)| dt = \frac{m_c}{\kappa(T)} \equiv Q_0(T) \ . \tag{2.4}$$

Thus, once a charge $Q_0(T)$ has flowed through the wire, it fails irreversibly and becomes an insulator. The charge $Q_0(T)$ depends on the temperature. It has been found experimentally that the product DZ^*e has an Arrhenius temperature dependence:[4] $DZ^*e \propto \exp(-\Delta E/k_B T)$. Typically, ΔE is comparable to the activation energy for grain boundary diffusion. Since ρ is proportional to T for metals at room temperature and N_a varies slowly with T, to a good approximation $Q_0(T)$ has an Arrhenius temperature dependence as well. Thus, for a constant current I, Eq. (2.4) reduces to Eq. (1.1) with $n=1$, which is the empirical result in the low-current-density regime. Equation (2.4) is therefore an appropriate generalization of the empirical law Eq. (1.1) to the more general situation in which the current varies with time.

Note that the absolute value of the current appears in our failure criterion (2.4). This is because electromigration damage to a conducting wire cannot be repaired simply by reversing the current. Indeed, ac currents lead to electromigration failure in times comparable to dc currents of the same magnitude.

In our model, we take the resistance of each wire to be constant until it fails. In a real wire, the resistance decreases as a precursor to complete failure. This effect will be neglected in the interest of simplicity. Note, however, that the resistance of the network as a whole will vary in time, so a precursor to total failure is present in the behavior of the entire system. In our model the resistance decrease that foreshadows complete failure is a collective effect, which occurs as a result of successive failures of the microscopic constituents of the system.

Consider the behavior of an $N \times N$ random network of this type when subjected to a constant applied voltage V_{ext}. Some wires—those in isolated clusters, for instance—carry no current and so never fail. At some time t_1, one of the current-carrying bonds fails, and the resistance of the network increases discontinuously. More and more wires fail as time passes. At a time $T_f \ge t_1$, the last conducting pathway across the system breaks and electrical failure is complete.

To perform a Monte Carlo simulation of this failure process, Kirchhoff's laws are solved to yield the distribution of currents in the network. The wire that carries the

most current is the first to fail. After this failure, Kirchhoff's laws are solved once more, and the second wire to fail is identified using the failure criterion Eq. (2.4). This process of repeated solution of Kirchhoff's laws is continued until conduction ceases. In our simulations, the network conductivity and geometry were recorded after each failure event.

In our model, current crowding next to voids is explicitly taken into account, since Kirchhoff's laws are solved after each failure. In addition, no *ad hoc* assumptions about void shape are needed—indeed, void morphology and growth can be observed in the simulations and can be compared with experiment.

The disorder in our model is admittedly very idealized. However, it is known that many properties of percolating systems are universal. We therefore expect that many of the observations made for our simple model will carry over to the more complex systems studied by experimentalists. At the very least, this approach is a natural starting point for more realistic simulations of electromigration failure in disordered thin films. More general types of disorder will be considered in our future work.

Our model is similar to the random fuse model[23–27] in several respects. To be specific, in both problems a random resistor network undergoes irreversible electrical failure. There is an important difference between the two models, however: The random fuse model is not a kinetic model, since failure occurs instantaneously when the applied voltage is sufficiently large. In contrast, our model is truly kinetic, since we can follow the breakdown process as a function of time.

The fact that our model is truly kinetic sets it apart from almost all previously studied models of breakdown in random media and makes it worth studying from a purely theoretical standpoint.[50] A kinetic breakdown model has been introduced and studied by Sornette and Vanneste,[48,49] however. Their model describes the failure of fuse networks that burn out due to Joule heating. In their model, the temperature T of a fuse with resistance R carrying current I obeys the equation

$$dT/dt = R|I|^b - aT \ , \tag{2.5}$$

where a and b are nonnegative constants. The term $R|I|^b$ accounts for a generalized Joule heating of the fuse; for real fuses $b=2$. The second term on the right-hand side of Eq. (2.5) is the rate that heat is lost to the substrate. When the temperature of a fuse reaches a given threshold, it burns out irreversibly and becomes an insulator.

Clearly, for $a=0$ and $b=1$, the more general failure criterion of Sornette and Vanneste reduces to ours if the temperature T is replaced by the charge $Q(t)=\int_0^t |I(t')|dt'$. Note, however, that Sornette and Vanneste did not actually study this case. As we shall see, it is possible to make significant progress analytically on this special case, and so it is of particular interest. In addition, Sornette and Vanneste adopted a different probability distribution for the resistance R than we have chosen, and did not apply their model to electromigration.

III. GROWTH OF A SINGLE CRACK

In this section, we begin work on our model by studying the growth of a single "crack" in a two-dimensional grid. Using a continuum approximation, we obtain the asymptotic behavior of the crack tip velocity in a network of infinite size. We also perform simulations of the growth of a single crack, and compare the results of these simulations with our predictions.[51]

Consider a square grid with lattice spacing a. Let N_x be the number of sites in the x direction and let N_y be the number of sites in the y direction. Thus, the coordinates (x,y) of the sites in the grid are (ma,na), where $m=0,1,\ldots,N_x-1$ and $n=0,1,\ldots,N_y-1$. Each bond in the lattice is a conductor with conductance σ. We impose periodic boundary conditions along the x direction, so that the columns with $m=0$ and $m=N_x$ coincide. In addition, we place busbars on the rows $y=0$ and $y=(N_y-1)a$. A constant voltage difference $V_0=(N_y-1)v_0$ is applied across these two busbars starting at time $t=0$.

Clearly, all of the horizontal bonds in the grid carry zero current. Each of the vertical bonds carries current σv_0 until failure occurs. All of the vertical bonds fail simultaneously at time $t=Q_0/(\sigma v_0)$.

Now consider the next level of complexity: Suppose that at time $t=0$ there is a single horizontal crack of length $2l_0 a$ in the center of the network. Specifically, consider the row of vertical bonds with their centers at height $y=Y$. Here Y is $N_y a/2$ if N_y is odd and is $(N_y-1)a/2$ if N_y is even. We assume that initially $2l_0+1$ consecutive vertical bonds in this row are "broken," i.e., they have zero conductance. Since we have imposed periodic boundary conditions in the x direction, the horizontal placement of this crack is immaterial. For definiteness, we shall assume that the x coordinates of the broken bonds are $X-l_0a, X-l_0a+a,\ldots,X+l_0a-a, X+l_0a$. Here X is $N_x a/2$ if N_x is even and is $(N_x-1)a/2$ if N_x is odd. None of the other bonds in the network are broken at $t=0$.

The current distribution is altered dramatically from the uniform current distribution that prevails when there is no crack present. For example, consider a resistor network with $N_x=N_y=128$ in which there is a crack of length 12. Figure 1 shows the currents in the vertical bonds with their centers at height $y=Y$, as well as the currents in the horizontal bonds with height $y=Y-a/2$. Clearly, the closer a conductor is to one of the crack tips, the larger the current that flows through it. The current enhancement is largest in the two unbroken vertical conductors adjacent to the crack tips, and as a result, these are the first bonds to fail. The subsequent behavior of the crack is less obvious, since the failure process in our model is a cumulative effect. Our simulations show that at all times, the next bonds to fail are the vertical bonds immediately adjacent to the crack tips. Thus, the crack tips propagate laterally until they meet and network failure is complete. The vertical bonds with their centers at heights $y\neq Y$ and all of the horizontal bonds remain conducting throughout the failure process. Our simulations

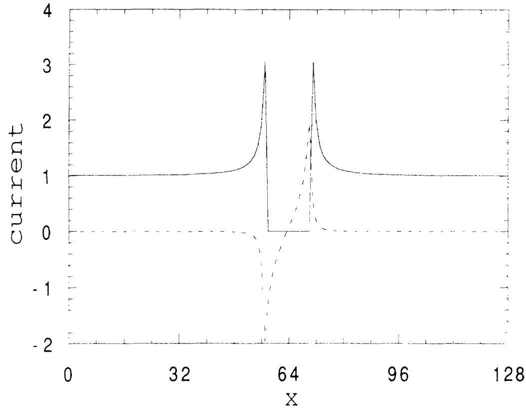

FIG. 1. The current distribution in a resistor network with $N_x = N_y = 128$ in which there is a crack of length $2l_0 = 12$. We have set σ, v_0, and a to 1. The currents through the vertical bonds with their centers at height $y = Y$ are shown with a full curve. The dashed curve gives the currents through the horizontal bonds with height $y = Y - a/2$. The x coordinate of a horizontal bond is measured from its midpoint, and we have adopted the convention that a horizontal current flowing to the right is positive.

strongly suggest that these observations apply for all values of N_x, N_y, and l_0. Although damage is done to all of the bonds in the network, only vertical bonds with centers at height $y = Y$ accumulate sufficient damage that they fail before current ceases to flow entirely.

Let us consider the crack tip velocity as a function of time. As the crack grows, the resistance of the network increases. If the externally applied voltage V_0 is constant, the net current I_0 flowing through the network will decrease with the passage of time. Therefore, the crack dynamics depends on whether V_0 or I_0 is held fixed. As we shall see, the fixed current problem is much simpler than the fixed voltage problem, and all of the results obtained in this paper pertain to the fixed current problem. There is an additional motivation for studying the fixed current case: In most of the experimental work on the lifetime of current-carrying wires performed to date, the external current was constant. For the remainder of the paper, we assume that the total current I_0 flowing through the network is constant until the network as a whole has failed.

We can readily write down an equation of motion for the crack tips. Suppose that the crack length is $2la$ at a given time. Let $I(n,l)$ denote the current flowing through the vertical bond that is a distance na to the right of the crack center and that has its center at height $y = Y$. Further, let t_n be the time when this bond fails, and we adopt the convention that $t_{l_0} = 0$. Finally, we set $\Delta t_n = t_{n+1} - t_n$ for $n \geq l_0$. The equation of motion is

$$\sum_{l=l_0}^{n-1} I(n,l)\Delta t_l = Q_0 , \tag{3.1}$$

where $n > l_0$. Equation (3.1) simply states that the nth bond fails once the net amount of charge that has flowed through it is Q_0. Note that the direction of the current through the vertical bonds never changes, and so it is not necessary to write $|I(n,l)|$ in lieu of $I(n,l)$ in Eq. (3.1).

Although Eq. (3.1) is readily solved numerically for finite grids, we have not succeeded in solving it exactly for all times. We have been able to make progress analytically, however, using a continuum approximation to study the growth of a crack in an infinitely large grid. If the initial length of the crack is large, the discrete lattice structure has little effect on the crack dynamics. Even if the initial length of the crack is comparable to the lattice spacing, the lattice structure becomes unimportant once the crack has grown to sufficient size. In both of these circumstances, a continuum approximation to the equation of motion may be applied. To obtain such an approximate equation of motion, we let the lattice spacing a approach zero, while keeping $L_x \equiv N_x a$, $L_y \equiv N_y a$, $x_0 \equiv l_0 a$, and $q_0 \equiv Q_0/a$ fixed. In this limit, the height of the crack shrinks to zero. Equation (3.1) becomes

$$\int_0^t j_y(x(t), x(t'), L_x, L_y)\,dt' = q_0 . \tag{3.2}$$

Here $2x(t)$ is the length of the crack at time t, and $j_y(x,x',L_x,L_y)$ is the vertical component of the current density at the point a distance x to the right of the crack center when the crack has length $2x'$.

Consider an infinitely large grid with a single crack of initial length $2l_0 a$. We assume that a constant external current flows through the film and that the continuum approximation (3.2) may be applied. For an infinitely large grid, the current density

$$j_y(x,x') \equiv j_y(x, x', L_x = \infty, L_y = \infty)$$

can be calculated analytically in the continuum approximation and has the following form:[25]

$$j_y(x,x') = \frac{j_0}{\sqrt{1-(x'/x)^2}} . \tag{3.3}$$

Here j_0 is the current density far from the crack.

Let $v_\infty(x,x_0)$ be the speed of the crack tips when the crack's length is $2x$. (The initial length of the crack is $2x_0$.) We will determine the behavior of $v_\infty(x,x_0)$ for $x \gg x_0$. We first introduce the new variable of integration $x' \equiv x(t')$. Equation (3.2) becomes

$$\int_{x_0}^x j_y(x,x')[v_\infty(x',x_0)]^{-1}dx' = q_0 . \tag{3.4}$$

Since x_0 is the only length scale in the problem, it makes sense to introduce the dimensionless widths $w \equiv x/x_0$ and $w' \equiv x'/x_0$. Applying these definitions and Eq. (3.3) in Eq. (3.4), we obtain

$$\int_1^w \frac{x_0\,dw'}{v_\infty(x_0 w', x_0)\sqrt{1-(w'/w)^2}} = \frac{q_0}{j_0} . \tag{3.5}$$

The quantity $q_0 v_\infty(x,x_0)/(j_0 x_0)$ is a dimensionless function of x and x_0. Since x_0 is the only length scale in the problem, $q_0 v_\infty(x,x_0)/(j_0 x_0)$ cannot depend on x and x_0 separately: It can only depend on their ratio x/x_0. Thus, we have the scaling form

$$v_\infty(x,x_0)=\frac{j_0x_0}{q_0}f\left[\frac{x}{x_0}\right], \qquad (3.6)$$

where f is a dimensionless function of x/x_0.

To learn something of the scaling function f, we solved Eq. (3.4) numerically using a finite difference approximation. In Fig. 2, $\log_{10}[q_0v(x,x_0)/(j_0x_0)]$ is plotted against $\log_{10}(x/x_0)$. The curve rapidly becomes linear as x/x_0 is increased, showing that

$$f(w)\sim Kw^\alpha \qquad (3.7)$$

for $w \gg 1$. Here K is a finite, nonzero constant independent of both x and x_0. Figure 2 also shows that the exponent α is close to 2. A linear least-squares fit to the curve for $x/x_0 \geq 10$ yields $\alpha=2.001\,20\pm0.000\,01$. The error quoted here does not take into account the fact that the slope of the curve slowly decreases with $\log_{10}(x/x_0)$. If the curve is fit for $x/x_0 \geq 20$, for example, a value of α still closer to 2 results.

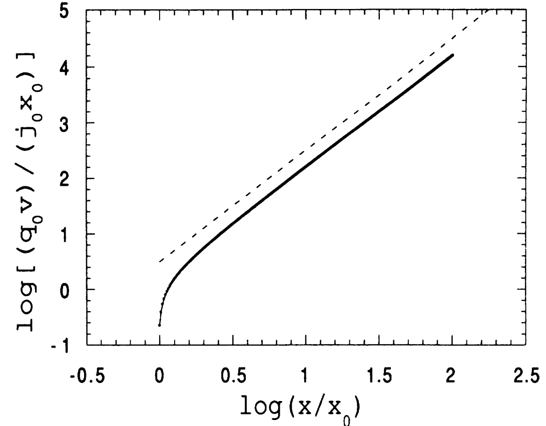

FIG. 2. $\log_{10}[q_0v(x,x_0)/(j_0x_0)]$ plotted vs $\log_{10}(x/x_0)$ (solid curve). The dashed line has a slope of 2.

Inspired by these numerical results, we assume that Eq. (3.7) is valid, and that $1<\alpha<3$. We shall now demonstrate that once these assumptions have been made, it follows that α must be *exactly* equal to 2.

Let $z=w'/w$. Using Eq. (3.6), we can rewrite Eq. (3.5) as follows:

$$\int_{1/w}^{1}\frac{w\,dz}{f(wz)\sqrt{1-z^2}}=1\ . \qquad (3.8)$$

We cannot simply replace $f(wz)$ in this integral by $Kw^\alpha z^\alpha$ because wz is not large throughout the range of integration. Corrections to the asymptotic scaling form (3.7) must therefore be taken into account. By assumption, $w^\alpha[f(w)]^{-1}$ tends to a finite constant K^{-1} as w tends to infinity. For large but finite w, there will be corrections to this leading-order behavior. These corrections will become increasingly important as w is decreased. It is therefore natural to assume that

$$w^\alpha[f(w)]^{-1}=\sum_{n=0}^{\infty}A_nw^{-n}\ , \qquad (3.9)$$

for all $w\geq 1$. Note that $A_0=1/K$. Inserting Eq. (3.9) into (3.8), we have

$$w^{1-\alpha}\sum_{n=0}^{\infty}A_nw^{-n}\int_{1/w}^{1}\frac{dz}{z^{\alpha+n}\sqrt{1-z^2}}=1\ . \qquad (3.10)$$

We now analyze the integrals that appear on the right-hand side of Eq. (3.10). Using our assumption that $1<\alpha<3$, we obtain

$$\int_{1/w}^{1}\frac{dz}{z^{\alpha+n}\sqrt{1-z^2}}=\frac{w^{\alpha+n-1}}{\alpha+n-1}+C_n(\alpha)+O(w^{\alpha+n-3})\ , \qquad (3.11)$$

for $w \gg 1$. Here

$$C_n(\alpha)\equiv\int_0^1\left[\frac{1}{\sqrt{1-z^2}}-\sum_{l=0}^{[n/2]}(-1)^l\begin{bmatrix}-1/2\\ l\end{bmatrix}z^{2l}\right]\frac{dz}{z^{\alpha+n}}+\sum_{l=0}^{[n/2]}(-1)^l\begin{bmatrix}-1/2\\ l\end{bmatrix}\frac{1}{2l+1-\alpha-n}(1-\delta_{2l+1-\alpha-n,0}) \qquad (3.12)$$

is a constant. In Eq. (3.12), $[x]$ denotes the smallest integer greater than or equal to x and the Kronecker delta $\delta_{m,n}$ is 1 if $m=n$ and is zero otherwise. Note as well that for the special case $\alpha+n=3$, the correction term of order $w^{\alpha+n-3}$ in Eq. (3.11) must be replaced by a term of order ln w.

Substituting the asymptotic form (3.11) in Eq. (3.10), we find that

$$\sum_{n=0}^{\infty}\frac{A_n}{\alpha+n-1}+A_0C_0(\alpha)w^{1-\alpha}+O(w^{-\beta})=1 \qquad (3.13)$$

for $w \gg 1$. Here β is the smaller of α and 2. We see that we must have

$$\sum_{n=0}^{\infty}\frac{A_n}{\alpha+n-1}=1 \qquad (3.14)$$

and that

$$C_0(\alpha)=0\ . \qquad (3.15)$$

Equation (3.15) uniquely specifies the value of α, as we shall now demonstrate. Explicitly,

$$C_0(\alpha)\equiv\int_0^1\left[\frac{1}{\sqrt{1-z^2}}-1\right]\frac{dz}{z^\alpha}-\frac{1}{\alpha-1}\ .$$

$C_0(\alpha)$ is an increasing function of α for $1<\alpha<3$, and $C_0(2)=0$. Thus, Eq. (3.15) has a single root on the inter-

val $1<\alpha<3$, and this root occurs at $\alpha=2$. We conclude that α is exactly 2, and that for $x \gg x_0$,

$$v_\infty(x,x_0) \cong \frac{Kj_0}{q_0 x_0} x^2 . \quad (3.16)$$

In our model, the crack tips accelerate as the length of the crack grows. Initially, the crack tips do not move as damage accumulates in the network. The crack tips move with increasing speed after the first bonds are broken. This acceleration occurs because the current crowding at the crack tips becomes more marked with the passage of time, and because the damage to the bonds is cumulative.

We handled the lower limit of integration with special care in our analysis of our equation of motion [Eq. (3.4)]. Care was needed because when $x \gg x_0$, the dominant contribution to the integral comes from x' close to x_0. This can be understood both from a mathematical and from a physical standpoint. We begin with the formal demonstration. The integrand in Eq. (3.11) has a nonintegrable singularity at $z=0$. As a result, the dominant contribution to this integral comes from z close to $1/w$, that is, from x' close to x_0. The same is also true of the equation of motion (3.8). We now turn to our heuristic explanation. Because the crack tips move slowly at first and then accelerate, most of the charge needed to break a bond flows through it while the crack tip is still far away. We again conclude that the dominant contribution to the integral on the left-hand side of Eq. (3.4) comes from x' relatively close to x_0.

The value of the constant $K=A_0^{-1}$ in Eq. (3.16) is determined by Eq. (3.14). Since the value of K depends on all of the A_n's with $n \ge 1$, we have not been able to determine its value. However, this is of little concern because we have been able to determine how the crack tip velocity grows with increasing crack length.

Now that we know the asymptotic behavior of $v_\infty(x,x_0)$, we can integrate to find the time dependence of the tip location x for $x \gg x_0$. Clearly,

$$t=\int_{x_0}^{x} \frac{dx'}{v_\infty(x',x_0)} . \quad (3.17)$$

Inserting Eqs. (3.6) and (3.9) in (3.17) and using the result $\alpha=2$, we obtain

$$\sum_{n=0}^{\infty} \frac{A_n}{n+1} \left[1-\left[\frac{x_0}{x} \right]^{n+1} \right] = \frac{j_0 t}{q_0} .$$

For $x \gg x_0$, this becomes

$$1-A_0 \left[\frac{x_0}{x} \right] \cong \frac{j_0 t}{q_0} ,$$

where we have employed Eq. (3.14) and the fact that $\alpha=2$. Finally, we have the desired result: For $x \gg x_0$

$$x \cong K^{-1} \frac{x_0}{1-j_0 t/q_0} . \quad (3.18)$$

Interestingly, Eq. (3.18) shows that the time to failure in the presence of the crack is q_0/j_0. This is the time it takes a defect-free film to fail, and so the presence of the crack does not reduce the lifetime of an infinitely large film. For a finite-sized film, of course, the lifetime will always be reduced by the presence of a crack. What we have shown is that this reduction tends to zero in the limit that the film dimensions become large compared to the initial length of the crack.

To test Eq. (3.16), we carried out simulations of the growth of a single crack in a square grid with $N_x=N_y=N$ and $a=1$. We shall briefly describe how these simulations were performed. Consider the situation at the time $t=t_n$. The conjugate gradient method was first used to solve the Green's-function formulation of Kirchhoff's laws.[52] This yielded the currents in the unbroken bonds. The exact equation of motion (3.1) was then solved to give the time interval Δt_n, and hence t_{n+1}. In all of our simulations, the total current I_0 passing through the network was held constant. Finally, we set I_0/N to 1 to facilitate comparisons between networks of different sizes.

In Fig. 3, $\log_{10}[q_0 v(l,l_0,N)/(j_0 l_0)]$ is plotted vs $\log_{10}(l/l_0)$ for $N=100$, 200, 400, and 600. In each case, $l_0=7$. For l in the interval $2l_0<l<N/3$, the function $\log_{10}[v(l,l_0,N)]$ is close to being linear in $\log_{10}(l/l_0)$. This lends further support to our supposition that $v_\infty(x,x_0)$ grows as a power of x for $x \gg x_0$. When l is small, the discrete lattice structure increases the slope of the curve. The slope of the curve also increases as $2l$ approaches N, when finite-size effects become important. This suggests that the best estimate of α for a given value of N is obtained by computing the minimum slope of the curve. Let this slope be $\alpha(N)$. Our data for $\alpha(N)$ are shown in Fig. 4. We extrapolated our data to $1/N=0$ by fitting to the form $\alpha(N)=a_0+a_1N^{-1}+a_2N^{-2}$ and so obtained an estimate of α corrected for finite-size effects. Our estimate $\alpha=2.003\pm0.004$ is in excellent agreement with our prediction that α is exactly 2.

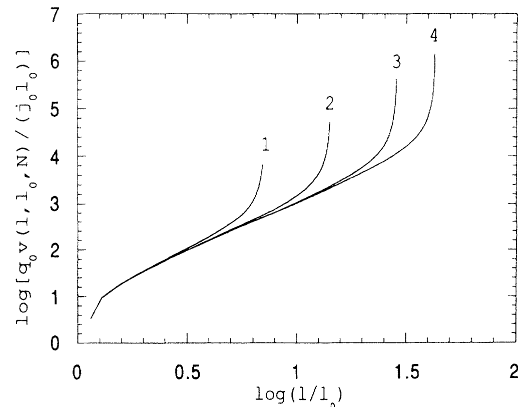

FIG. 3. $\log_{10}[q_0 v(l,l_0,N)/(j_0 l_0)]$ plotted vs $\log_{10}(l/l_0)$ for $N=100$ (curve 1), 200 (curve 2), 400 (curve 3), and 600 (curve 4). In each case, $l_0=7$.

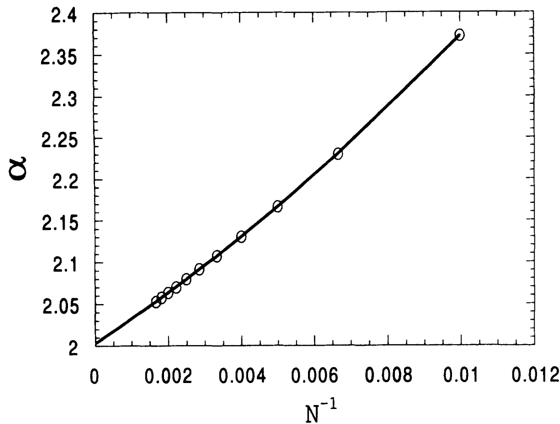

FIG. 4. Plot of $\alpha(N)$ vs $1/N$ (open circles). The fit to the data is shown using a solid curve.

IV. THEORY OF THE FAILURE TIME FOR FILMS WITH MULTIPLE CRACKS

The time that it takes a film to fail is probably the most obvious quantity we can choose to study in our model of electromigration failure. Moreover, it is the quantity of greatest interest in microelectronics applications. Accordingly, in this section we will study the failure time of networks with nonzero values of p.

As we saw in the preceding section, even the growth of a single crack is complex. The dynamical behavior of a film with many cracks must be complicated indeed, since the cracks interact and fuse as they grow. It is therefore quite surprising that analytical results can be obtained on the dependence of the failure time on p and L, as we shall show.

A. Lifshitz-type theory

In a series of important papers, Duxbury and coworkers developed a theory governing the failure voltage of a random fuse network[24–26] in which the defects are initially dilute. Duxbury *et al.* argued that the most critical defect in two dimensions is a line defect oriented perpendicularly to the direction of the ambient current. They then used a continuum approximation in which this line of insulators was replaced by an elliptical defect to find voltage required to initiate failure. Finally, the result of this calculation was combined with an estimate of the size of the largest defect present in the system to give the breakdown voltage. The predictions of this "Lifshitz-type" theory are in accord with the results of Monte Carlo simulations.

The success of the Lifshitz-type theory in explaining the behavior of random fuse networks suggests that it is a natural starting point for a theory of electromigration failure. In this short subsection, we develop a Lifshitz-type theory for the failure time.

We begin by determining the failure time for an $N\times N$ network with a single crack of initial length $2x_0=2l_0a$. If $a \ll x_0 \ll L$, the crack tip velocity will be given by Eq. (3.16) initially. As the crack tips approach the film boundaries, however, finite-size corrections to this result become increasingly important. Therefore, the failure time T_f is not given by the integral $\int_{x_0}^{L/2} v_\infty^{-1}(x',x_0)dx'$. Fortunately, it is a simple matter to determine the exact value of T_f. The total number of vertical conducting bonds that fail is $N-(2l_0+1)$. This is the number of conducting bonds that are in the same row as the crack at time $t=0$. The total charge that must flow through this row for all of these bonds to fail is $[N-(2l_0+1)]Q_0$. Thus, the failure time is given by

$$I_0T_f=[N-(2l_0+1)]Q_0 \ . \tag{4.1}$$

Note that a simple expression of this kind does not hold when the applied voltage is held fixed, since the current flowing through the network changes as a function of time in that case. This is why it is easier to develop a theory for the behavior of networks with fixed applied current.

Now consider an $N\times N$ network that has a fraction $p \ll p_c$ of insulating bonds at time $t=0$. In our approximate Lifshitz-type theory, we ignore interactions between cracks in the dilute limit $p \ll p_c$. In this approximation, each of the cracks grows horizontally, and network failure is complete when the tips of a crack meet. (Recall that periodic boundary conditions apply in the x direction.) Equation (4.1) shows that the crack whose growth leads to failure of the network is the one that is longest initially. Let the number of broken bonds in the longest crack at $t=0$ be $\nu_{\max}$. The mean failure time $\langle T_f\rangle$ is then

$$\langle T_f\rangle \cong \frac{Q_0}{I_0}(N-\langle \nu_{\max}\rangle) \ . \tag{4.2}$$

Equation (4.2) relates the mean failure time to a relatively simple geometrical quantity, the mean number of bonds in the longest crack $\langle \nu_{\max}\rangle$. It is not difficult to determine the behavior of $\langle \nu_{\max}\rangle$ in certain limits. For example, for a given value of $p<p_c$, the average value of $\nu_{\max}$ grows as

$$\langle \nu_{\max}\rangle \sim a(p)\ln N \ , \tag{4.3}$$

as $N\to\infty$.[25] Here $a(p)$ is a constant that tends to zero as $|\ln p|^{-1}$ as $p\to 0$.

The result of our Lifshitz-type theory [Eq. (4.2)] applies only when the fusion of two cracks to form a single larger crack is unlikely. As we shall show, this means that the Lifshitz theory is a good approximation only when $pN \ll 1$. Our Monte Carlo simulations (which are described in detail in Sec. V) do agree with Eq. (4.2) for $p \ll N^{-1}$. However, for larger values of p, the prediction of the Lifshitz theory differs markedly from the $\langle T_f\rangle$ values obtained in the simulations. This is because crack fusion grows more probable with increasing p, and it cannot be neglected as it is in the Lifshitz theory.

To take crack-crack interactions and the fusion of cracks into account, we need to employ a different approach. This is the subject of the next and subsequent subsections.

B. Heuristic estimate of the failure time

We have seen that the failure time can be computed exactly when there is a single crack present initially. In the following, we successively generalize this observation.

Suppose that initially there are $N-n$ insulating vertical bonds in one row of the lattice, and that there are no other insulating bonds at time $t=0$. In general, the insulating bonds will not be contiguous, and multiple cracks will be present. Failure is complete once a total charge nQ_0 has flowed through the row that contains these cracks. The failure time is therefore $T_f=nt_0$, where the constant $t_0 \equiv Q_0/I_0$ has units of time. Notice that although this result is readily obtained, the task of actually determining how the cracks grow and fuse would be daunting indeed.

Let us next contemplate a slightly more complex problem: Suppose that at time $t=0$ there are $N-n_1$ broken vertical bonds in one row and that there are $N-n_2$ broken vertical bonds in a second row. We assume that no other bonds are broken initially, that the distance between the two rows is much larger than a, and that $n_1 \neq n_2$. For initial configurations of this kind, we expect that the current will flow downward through each of the conducting vertical bonds in rows 1 and 2 throughout the failure process. This was true for all of the initial configurations we studied, and we assume it to be generally true. Since the distance between the two rows is large, the cracks all grow laterally until all of the bonds in one of the rows are insulating. The time needed for all the conducting bonds in the ith row to fail is $T_i=n_i t_0$, where $i=1,2$. This result holds provided that the current flow is not interrupted before the ith row fails. For example, if row 1 fails first, the second row will never fail. We conclude that T_f is the smaller of $n_1 t_0$ and $n_2 t_0$, i.e.,

$$T_f=\min(n_1,n_2)t_0 \ . \tag{4.4}$$

Note that the assumption that the rows are sufficiently far apart is needed to ensure that the cracks grow horizontally. If the rows are too close together, some horizontal bonds could be broken, and our result (4.4) may not apply.

These examples suggest how we may generalize to an arbitrary initial configuration of insulating bonds C. Let Γ be a closed self-avoiding path defined on the dual lattice (Fig. 5). Γ may be any closed self-avoiding path that wraps around the lattice once before closing. For convenience, in what follows we will refer to such a self-avoiding path as simply "a path." We now assign a "length" $n(\Gamma)$ to Γ: We let $n(\Gamma)$ be the total number of conducting bonds that cross the path Γ at time $t=0$. The path with the smallest value of n (the "shortest path") will be denoted Γ_s.

Once the network has failed, there exists a path that is crossed only by insulating bonds. We will call such a path a critical path. In general, there will be more than one critical path. In the examples studied so far, the critical path is unique, and is simply a straight line traversing the network from left to right. For an arbitrarily chosen

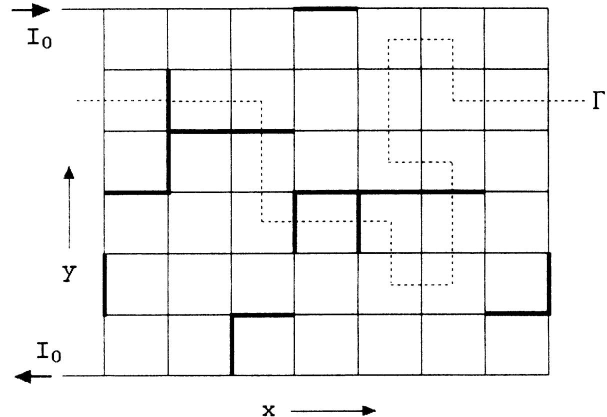

FIG. 5. The initial configuration of a 7×7 network. Conducting bonds are shown in full lines, and insulating bonds are shown with bold full lines. A closed self-avoiding path Γ on the dual lattice is shown with dashed lines. The length of the path is $n(\Gamma)=12$. Note that periodic boundary conditions apply in the x direction, and so the columns to the far left and right coincide.

initial configuration C, the critical path could be much more complex and may not be unique.

In our example in which bonds are initially broken in two rows, the critical path lies in the row with the smallest value of n_i. Thus, the critical path Γ_c is the shortest-path Γ_s, i.e.,

$$n(\Gamma_c) \leq n(\Gamma) \tag{4.5}$$

for all paths Γ. In addition, the failure time is

$$T_f=n(\Gamma_s)t_0 \ . \tag{4.6}$$

Equations (4.5) and (4.6) also hold in our first example.

This suggests the following speculation: Perhaps the critical path Γ_c is a shortest path Γ_s for an *arbitrary* initial configuration C, and perhaps the failure time is always given by Eq. (4.6). Actually, this speculation is not quite correct, but it is close to being right. We shall argue that the length of the critical path $n(\Gamma_c)$ is almost always close to the length of the shortest path $n(\Gamma_s)$. Moreover, we will show that for any initial configuration C, the failure time T_f is never greater than $n(\Gamma_s)t_0$. Most significantly, we argue that the mean failure time $\langle T_f \rangle$ is very close to being equal to $\langle n(\Gamma_s) \rangle t_0$. (The angular brackets denote an average over initial configurations C.)

Before giving arguments for these assertions, let us discuss their value. Simulations of our model of electromigration are extremely time consuming, since Kirchhoff's equations for the network must be repeatedly solved. However, if we are content with knowing the approximate failure time, Kirchhoff's equations need never be solved: It is sufficient to compute the shortest-path length, and this can be done easily and with great speed.[53] Moreover, as we discuss in Sec. IV E, much is known about the mean length of the shortest path in certain limits, and this knowledge can be directly applied to our

model. Our speculation relates the time that a complex dynamical process comes to an end to a simple geometrical quantity, the length of the shortest path through the initial configuration.

We now present a heuristic argument for the speculation that Eqs. (4.5) and (4.6) are correct for arbitrary initial configurations C. (Later we will give a more precise treatment, but the heuristic argument is instructive, and so we will give it.) Consider an arbitrary path Γ that traverses a given initial configuration C. We shall assign a failure time $t(\Gamma)$ to this path. Physically, $t(\Gamma)$ is the time that it would take for all of the conducting bonds that cut Γ to fail if the current flow through this path were not interrupted by the failure of bonds elsewhere in the network. We define $t(\Gamma)$ formally as follows. At time $t=0$, the current flow begins and, after a time, conducting bonds begin to break. The network as a whole fails at time $t=T_f$. If all of the bonds that cut Γ are insulators at this time, $t(\Gamma)$ is set equal to T_f. Otherwise, all of the bonds that do not cut Γ are replaced by conductors with unchanging conductance σ. The bonds that cut Γ are unaltered. The current flow is then restarted, and conducting bonds that cut Γ again start to fail. Ultimately, the last conducting bond that crosses Γ breaks at a time we define to be $t(\Gamma)$. Note that by definition,

$$T_f=t(\Gamma_c) . \tag{4.7}$$

Moreover,

$$t(\Gamma_c)\le t(\Gamma) \tag{4.8}$$

for all paths Γ.

To complete our argument, we must estimate $t(\Gamma)$. We assume that once a charge has crossed Γ, it never recrosses this path. Thus, we neglect the possibility that the current flow "backtracks" across Γ. With this assumption, we have $I_0 t(\Gamma)=n(\Gamma)Q_0$ or $t(\Gamma)=n(\Gamma)t_0$. This is because all charges that are injected into the network cross Γ once, and because a charge Q_0 is required to break each of the conducting bonds that cut this path. Equation (4.8) then shows that $n(\Gamma_c)\le n(\Gamma)$ for all paths Γ. This means that the critical path Γ_c is a shortest path. Furthermore, Eq. (4.7) becomes Eq. (4.6).

This argument does not yield exact results because backtracking was neglected in estimating $t(\Gamma)$. Note, however, that if backtracking does occur, it reduces the value of $t(\Gamma)$ below $n(\Gamma)t_0$. This is because charges that backtrack damage three or more conducting bonds that cut Γ, not just one. Thus, Eq. (4.6) may overestimate the failure time. Formally, we have

$$T_f\le n(\Gamma_s)t_0 . \tag{4.9}$$

Although we have given a somewhat intuitive argument for the inequality (4.9), we can give a rigorous demonstration of its validity as follows: Consider an arbitrary path Γ at time t. We walk along the path from left to right, and each time we arrive at a new bond we assign a sign to the current in the bond. If the current passing through the bond goes from left to right across the path, it is a positive current; otherwise, it is a negative current. Let us index the conducting bonds that cut Γ at time $t=0$ by the integers $k=1,2,\dots,n(\Gamma)$. Because charge is conserved, for any time $t<T_f$ we have

$$\sum_{k=1}^{n(\Gamma)} i_k(t)=I_0 . \tag{4.10}$$

Here $i_k(t)$ is the current passing through the kth bond at time t, and has the appropriate sign. Taking the absolute value of this relation and setting $\Gamma=\Gamma_s$, we obtain

$$\sum_{k=1}^{n(\Gamma_s)} |i_k(t)|\ge I_0 . \tag{4.11}$$

Let $t^*\equiv n(\Gamma_s)t_0$. If the network fails before time t^*, our assertion is proved. Therefore, we suppose that this is not the case, and consider the situation at time t^*. Integrating Eq. (4.11) from $t=0$ to t^*, we obtain

$$\sum_{k=1}^{n(\Gamma_s)} \int_0^{t^*} |i_k(t)|dt\ge Q_0 n(\Gamma_s) . \tag{4.12}$$

Since a conducting bond fails once a charge Q_0 has flowed through it, $\int_0^{t^*}|i_k(t)|dt\le Q_0$ for all k. Equation (4.12) shows that the only way that this can be so is for $\int_0^{t^*}|i_k(t)|dt$ to be equal to Q_0 for all k. This means that the network fails at time t^*. We conclude that $T_f\le t^*=n(\Gamma_s)t_0$, and our result (4.9) is proven.

C. Variation formulation

In this section, we will develop a variational formulation of our problem. This will allow us to improve upon the simple heuristic arguments given in the preceding section. Ultimately, we will use the variational formulation to argue that $\langle T_f\rangle$ is to a good approximation equal to $\langle n(\Gamma_s)\rangle t_0$.

Consider a path Γ that traverses a given initial configuration C. We divide the bonds that are initially conducting and that cross Γ into three groups. Group 1 consists of the bonds that carry nonnegative currents at all times, while group 2 contains the bonds that always carry currents that are negative or zero. (If a conductor never carries any current, we place it in group 1.) The bonds that carry both positive and negative currents before time $t=T_f$ make up group 3.

Let $n^+(\Gamma,t)$ be the number of bonds in group 1 that are still conducting at time t, and define $n^-(\Gamma,t)$ and $n^0(\Gamma,t)$ analogously. We number the bonds in group 1 as follows: The bonds that never break are labeled by the integers $1,2,\dots,n^+(\Gamma,T_f)$. (The ordering of these bonds is unimportant.) The ith bond in group 1 to break is assigned the number $n^+(\Gamma,0)-i+1$. The bonds in groups 2 and 3 are numbered in the same way. Finally, let $n(\Gamma,t)$ be the total number of conducting bonds that cross Γ at time t, so that

$$n(\Gamma,t)=n^+(\Gamma,t)+n^-(\Gamma,t)+n^0(\Gamma,t) . \tag{4.13}$$

Note that $n(\Gamma,0)=n(\Gamma)$.

Let $i_k^+(\Gamma,t)$, $i_k^-(\Gamma,t)$, and $i_k^0(\Gamma,t)$ denote the current in the kth conductor in groups 1, 2, and 3, respectively. By

charge conservation, the total current passing through path Γ at time t is equal to I_0:

$$\sum_{k=1}^{n^+(\Gamma,t)} i_k^+(\Gamma,t) + \sum_{k=1}^{n^-(\Gamma,t)} i_k^-(\Gamma,t) + \sum_{k=1}^{n^0(\Gamma,t)} i_k^0(\Gamma,t) = I_0 \ . \tag{4.14}$$

If a bond in group 1 is broken before time T_f, the net charge that passes through it is Q_0. Thus, if $k > n^+(\Gamma, T_f)$,

$$\int_0^{T_f} i_k^+(\Gamma,\tau)d\tau = Q_0 \ . \tag{4.15}$$

In the same way, if $k > n^-(\Gamma, T_f)$, then

$$\int_0^{T_f} i_k^-(\Gamma,\tau)d\tau = -Q_0 \ . \tag{4.16}$$

The situation is more complicated for bonds in group 3. If the kth bond in group 3 breaks before time T_f, the net charge that passes through it is less than Q_0 and greater than $-Q_0$. We define $Q_k^+(\Gamma)$ to be the total charge that flows through the kth bond when the current is positive. Similarly, let $-Q_k^-(\Gamma)$ be the total charge that passes through the kth conductor when the current is negative. The failure criterion (2.4) becomes

$$\int_0^{T_f} |i_k^0(\Gamma,\tau)| d\tau = Q_k^+(\Gamma) + Q_k^-(\Gamma) = Q_0 \ . \tag{4.17}$$

Integrating Eq. (4.14) from time 0 to time t and using Eqs. (4.15) and (4.16), we obtain

$$I_0 t = Q_0[n^+(\Gamma,0) - n^+(\Gamma,t)] - Q_0[n^-(\Gamma,0) - n^-(\Gamma,t)] + \sum_{k=n^0(\Gamma,t)+1}^{n^0(\Gamma,0)} [Q_k^+(\Gamma) - Q_k^-(\Gamma)]$$
$$+ \sum_{k=1}^{n^+(\Gamma,t)} q_k^+(\Gamma,t) - \sum_{k=1}^{n^-(\Gamma,t)} q_k^-(\Gamma,t) + \sum_{k=1}^{n^0(\Gamma,t)} q_k^0(\Gamma,t) \ , \tag{4.18}$$

where

$$q_k^+(\Gamma,t) \equiv \int_0^t i_k^+(\Gamma,\tau)d\tau \ , \tag{4.19a}$$

$$q_k^-(\Gamma,t) \equiv -\int_0^t i_k^-(\Gamma,\tau)d\tau \ , \tag{4.19b}$$

and

$$q_k^0(\Gamma,t) \equiv \int_0^t i_k^0(\Gamma,\tau)d\tau \ . \tag{4.19c}$$

We now divide $q_k^0(\Gamma,t)$ into two parts. The first part is the charge that flows through the kth bond in group 3 when the current is positive, $q_k^{0,+}(\Gamma,t)$. The second part is the charge that flows through this bond when the current is negative, $-q_k^{0,-}(\Gamma,t)$. With these definitions, we have

$$q_k^0(\Gamma,t) = q_k^{0,+}(\Gamma,t) - q_k^{0,-}(\Gamma,t) \ . \tag{4.20}$$

Using Eqs. (4.13), (4.17), and (4.20), we may rewrite Eq. (4.18) as follows:

$$F(\Gamma,t) - I_0 t = \sum_{k=1}^{n^+(\Gamma,t)} [Q_0 - q_k^+(\Gamma,t)] + \sum_{k=1}^{n^-(\Gamma,t)} [Q_0 - q_k^-(\Gamma,t)] + \sum_{k=1}^{n^0(\Gamma,t)} [Q_0 - q_k^{0,+}(\Gamma,t) - q_k^{0,-}(\Gamma,t)] \ , \tag{4.21}$$

where

$$F(\Gamma,t) \equiv Q_0 n(\Gamma,0) - 2Q^-(\Gamma,t) \tag{4.22}$$

and

$$Q^-(\Gamma,t) \equiv \sum_{k=n^-(\Gamma,t)+1}^{n^-(\Gamma,0)} Q_0 + \sum_{k=n^0(\Gamma,t)+1}^{n^0(\Gamma,0)} Q_k^-(\Gamma) + \sum_{k=1}^{n^-(\Gamma,t)} q_k^-(\Gamma,t) + \sum_{k=1}^{n^0(\Gamma,t)} q_k^{0,-}(\Gamma,t) \ . \tag{4.23}$$

Let us pause to discuss this result. The sums on the right-hand side of Eq. (4.21) run over all the conducting bonds that cross Γ at time t, and the quantity on the right-hand side is just the total charge that must still flow through these bonds for them all to be broken. Now consider the left-hand side of Eq. (4.21). $Q_0 n(\Gamma,0)$ is the total amount of charge that is needed to break all of the conducting bonds that cross Γ at time $t=0$. $Q^-(\Gamma,t)$ is the total amount of charge that recrosses the path Γ before time t, i.e., it is the charge that has crossed Γ due to negative "backtracking" currents. [Note that charges that return to the region above Γ twice contribute twice to $Q^-(\Gamma,t)$.] Each time that a charge returns to the region above Γ, it damages conducting bonds twice—once

when it backtracks, and again when it returns to the region beneath Γ. Thus, at time t the total amount of charge that has done damage to the bonds crossing Γ is $I_0 t + 2Q^-(\Gamma,t)$. The first term in this expression is the total charge that flowed across Γ for the first time, and the second is the remaining charge that flowed across the path before time t. We conclude that the left-hand side of Eq. (4.21) is the charge needed to break the remaining conducting bonds that cross Γ, and so the two sides of the equation indeed coincide.

All of the terms in brackets on the right-hand side of Eq. (4.21) are nonnegative. Thus, we have the following inequality, valid for any time t and path Γ:

$$I_0 t \le F(\Gamma,t) \ . \tag{4.24}$$

We now set t to the failure time T_f in this result. This gives

$$I_0 T_f \le F(\Gamma,T_f) \ . \tag{4.25}$$

Because all the bonds in the critical path are insulating at time T_f, the right-hand side of Eq. (4.21) vanishes for $t = T_f$ and $\Gamma = \Gamma_c$. Thus

$$I_0 T_f = F(\Gamma_c,T_f) \ . \tag{4.26}$$

Substituting this into Eq. (4.25), we find that

$$F(\Gamma_c,T_f) \le F(\Gamma,T_f) \tag{4.27}$$

for all paths Γ.

Equation (4.27) shows that the critical path is the path Γ that minimizes the functional $F(\Gamma,T_f)$. Once the critical path has been found, the failure time can, in principle, be computed using Eq. (4.26). This is the variational formulation that we sought to derive.

Physically, $F(\Gamma,t) - I_0 t$ is just the charge that must still cross the path Γ after time t in order for all the conducting bonds that cut the path to fail. Clearly, then, $F(\Gamma_c,T_f) - I_0 T_f = 0$ and $F(\Gamma,T_f) - I_0 T_f > 0$ for any path Γ that is not critical. This is the basic physical content of the variational formulation.

It should be kept in mind that the currents flowing through the conducting bonds and the failure time T_f depend on the initial configuration C. To avoid confusion, from this point on we will explicitly display the dependence of the functional $F(\Gamma,T_f)$ on C. To this end, we set

$$F(\Gamma,C) \equiv F(\Gamma,T_f) \ . \tag{4.28}$$

For much the same reason, we write

$$Q^-(\Gamma,C) \equiv Q^-(\Gamma,T_f) \tag{4.29}$$

and

$$n(\Gamma,C) \equiv n(\Gamma,t=0) \ . \tag{4.30}$$

In our new notation, Eqs. (4.27) and (4.26) become

$$F(\Gamma_c,C) \le F(\Gamma,C), \quad \text{for all paths } \Gamma \tag{4.31}$$

and

$$I_0 T_f = F(\Gamma_c,C) \ . \tag{4.32}$$

The functional $F(\Gamma,C)$ is given by

$$F(\Gamma,C) = Q_0 n(\Gamma,C) - 2Q^-(\Gamma,C) \ . \tag{4.33}$$

In the heuristic theory developed in the preceding section, the effects of negative currents were neglected. If we simply set $Q^-(\Gamma,C)$ to zero in Eqs. (4.31)–(4.33), we recover the approximate results (4.5) and (4.6). Actually, the critical path does not necessarily minimize the length $n(\Gamma,C)$. Instead, it minimizes the more complex functional $F(\Gamma,C)$.

The functional $F(\Gamma,C)$ contains two parts. The first is the charge that must pass through Γ in order for all the conducting bonds that cross it at time $t=0$ to be broken. This term is proportional to the length $n(\Gamma,C)$ of the path, as defined in Sec. IV B. The second term $[2Q^-(\Gamma,C)]$ is twice the charge that crosses Γ due to the presence of negative currents. The critical path minimizes the functional $F(\Gamma,C)$, and represents a compromise between the effects of these two terms. The first term favors short paths. The second term, on the other hand, favors paths with large negative currents passing through them. Typically, these will be paths that are rather long. For example, when p is zero, paths Γ that cross a vertical line three or more times have appreciable values of $Q^-(\Gamma,C)$. These are paths with "overhangs." The larger the overhanging portions of the path are, the larger the value of $Q^-(\Gamma,C)$ will be. When p is small but nonzero, paths with large overhangs will usually have large values of $Q^-(\Gamma,C)$, just as they do when $p=0$.

Our variational formulation is not useful in numerical studies. This is because if we are to compute the functional $F(\Gamma,T_f)$, we must find the currents through all of the bonds in the network for all times $t \le T_f$. Once these currents have been calculated, both the failure time and the critical path are known, and there is no need whatsoever for the variational formulation. The real importance of the variational formulation is that it allows us to develop upper and lower bounds on the failure time. This is the subject of the next subsection.

D. Upper and lower bounds on the failure time

Using our variational formulation, we can readily obtain upper and lower bounds on the time to failure T_f. From Eqs. (4.31)–(4.33), we have

$$I_0 T_f \le Q_0 n(\Gamma,C) - 2Q^-(\Gamma,C)$$

for all paths Γ. In particular, this inequality holds for $\Gamma = \Gamma_s$, and so

$$I_0 T_f \le Q_0 n(\Gamma_s,C) - 2Q^-(\Gamma_s,C) \ . \tag{4.34}$$

This upper bound on T_f is an improvement on our earlier result (4.9), since $Q^-(\Gamma_s,C) \ge 0$. To obtain a lower bound, note that

$$I_0 T_f = Q_0 n(\Gamma_c,C) - 2Q^-(\Gamma_c,C) \ . \tag{4.35}$$

Since $n(\Gamma_s,C) \le n(\Gamma_c,C)$, we have

$$I_0 T_f \ge Q_0 n(\Gamma_s,C) - 2Q^-(\Gamma_c,C) \ . \tag{4.36}$$

Combining Eqs. (4.9) and (4.36), we have

$$Q_0 n(\Gamma_s,C) - 2Q^-(\Gamma_c,C) \le I_0 T_f \le Q_0 n(\Gamma_s,C) \; . \qquad (4.37)$$

Equation (4.37) shows that T_f is close to $n(\Gamma_s,C)t_0$ provided that $Q^-(\Gamma_c,C)$ is small. Thus, if backtracking through the critical path is negligible, Eq. (4.6) is close to being correct. This is an important conclusion, since it means that for Eq. (4.6) to be a good approximation, backtracking does not need to be negligible for all paths. Instead, it is enough for backtracking across the critical path Γ_c to be small.

In Sec. IV B we gave a heuristic argument for Eq. (4.6). In estimating the failure time $t(\Gamma)$ for a path Γ, we assumed that backtracking across Γ can be neglected. This assumption is definitely not valid for an arbitrary path Γ: Isolated bonds can be present even in the initial configuration C. Moreover, backtrack currents across certain types of paths can be substantial, as we have already noted. Our equality (4.37) shows that the assumption made in the heuristic treatment is much stronger than necessary, however: All that is needed is for backtracking across Γ_c to be small.

It is possible that $Q^-(\Gamma_c,C)$ is not negligible for certain special initial configurations C. To be precise, we shall argue that $Q^-(\Gamma_c,C)$ is small *on average*. This will allow us to conclude that

$$\langle T_f \rangle \cong \langle n(\Gamma_s,C) \rangle t_0 \; . \qquad (4.38)$$

We have not been able to prove rigorously that $\langle Q^-(\Gamma_c,C) \rangle$ is small. However, it is possible to argue convincingly that the effect of backtracking is modest for $p \ll p_c$ and for p close to p_c. Let us first discuss the limit of small p. If $p \ll N^{-2}$, in all likelihood there will be either zero or one broken bond in the network at time $t=0$. If there are no broken bonds initially, all of the vertical bonds break simultaneously. The critical path can therefore be taken to be any horizontal straight line that traverses the network. Since all of the vertical bonds carry the same positive current for $t \le T_f$, we must have $Q^-(\Gamma_c,C)=0$. If there is a single broken bond initially, on the other hand, the critical path is the horizontal straight line that contains this bond. A horizontal crack is nucleated by the broken bond, and the crack tips propagate laterally until they meet and the failure of the network is complete. Clearly, the currents flowing across the critical path are always positive, and again $Q^-(\Gamma_c,C)=0$.

The situation is more complex if p is small compared to p_c but is not small compared to N^{-2}. In this case, there are many broken bonds in the network at time $t=0$, although the broken bonds are initially dilute. At early times, cracks begin to grow laterally from the broken vertical bonds (Fig. 6). The broken horizontal bonds may nucleate cracks at somewhat later times, and the tips of these cracks also propagate horizontally. As the cracks grow larger, they begin to interact through the current flow, and at still later times, cracks may fuse. If two cracks are in the same row, their tips may meet, leading to the fusion of the two cracks and to the formation of a single larger crack. If two cracks are in adjacent rows, on

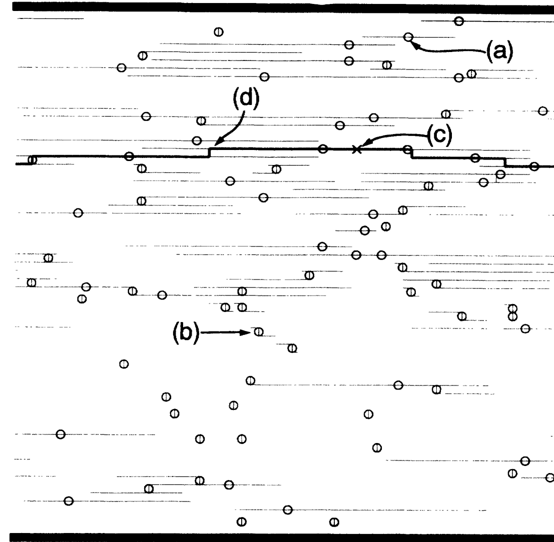

FIG. 6. The final and initial configurations of a 64×64 network with $p=0.01$. The bonds dual to bonds that are insulating in the final state are shown with solid lines. The critical path itself is shown with bold solid lines. Bonds that were broken at time $t=0$ are circled, and the busbars are shown with thick solid bars at the top and bottom of the network. The vertical bond (a) is broken initially, and leads to the formation of a crack whose tips propagate laterally. The horizontal bond (b) is insulating at time $t=0$, and it also nucleates a crack whose tips propagate laterally. Two cracks in the same row fused at point (c). A bridge between cracks in adjacent rows was formed at point (d).

the other hand, their tips normally pass one another traveling in the opposite direction—the cracks do not fuse when their tips are one lattice spacing apart. Instead, if the cracks do fuse, they do so through the formation of a "bridge" between them. A bridge is created when a single horizontal bond fails between the two cracks. Our simulations indicate that, almost invariably, two cracks fuse only if they are separated by at most one lattice spacing in the vertical direction (Fig. 6). Thus, the critical path Γ_c is composed of long, straight horizontal segments joined by an occasional vertical step of unit height.

Is backtracking across Γ_c ever important? Clearly, for early times it is not. In this instance, backtracking is absent if the broken bonds are remote from one another, just as it is when there is a single broken bond initially. Backtracking can only occur at early times if there are several nearby broken bonds, and this occurs with negligible probability. At late times, on the other hand, the current flow is constricted to flow through the few narrow apertures that remain in Γ_c. When the current flow is constricted in this way, it is most unlikely to backtrack. We conclude that, on average, negative currents across the critical path will be negligibly small for $p \ll p_c$.

Now consider the situation at the percolation threshold $p=p_c$. In most initial configurations C, there is a conducting bond whose removal disconnects the two bus-

bars, a so-called "singly connected bond" (SCB).[54] Up until time T_f, the SCB carries all of the current. The SCB is the only bond to break, and once it has broken, network failure is complete. In configurations of this kind, the critical path crosses only one conductor (the SCB), and there is never any backtracking. If there is no SCB in the initial configuration, it is practically certain that the simultaneous removal of two conducting bonds is sufficient to interrupt the flow of current.[54] These bonds are called "doubly connected bonds." In all but rather unusual initial configurations, the critical path crosses only two conductors, the doubly connected bonds. If this is the case, there is never any backtracking across the critical path. We conclude that at the percolation threshold $\langle Q^-(\Gamma_c,C)\rangle$ is small.

If p is close to but less than p_c, we must distinguish two cases. If L is much smaller than the correlation length ξ, the behavior of the network is essentially the same as if p were equal to p_c, and backtracking is again negligible. Suppose, on the other hand, that $L \gg \xi$. In the approximate nodes, links, and blobs picture,[55] the conducting backbone of a percolation cluster is composed of a network of quasi-one-dimensional "strings" or links that join a set of nodes whose typical separation is ξ. For simplicity, we shall take these nodes to form a square array. Each string consists of several sequences of singly connected bonds in series with thicker regions called "blobs," where there are two or more conducting bonds in parallel. The mean number of singly connected bonds in a string diverges as $(p_c-p)^{-1}$ as the percolation threshold is approached. The first bonds to fail are those on the hottest string. Once these have failed, the current increases in the vertical strings adjacent to the broken string, and these strings are likely to be the next to fail. In analogy with the behavior of a single crack in an otherwise defect-free network, we expect that the failure process of the disordered network will consist of the lateral propagation of a linear "crack." This crack is made up of a sequence of broken vertical strings, and its tips propagate until they meet. Thus, at least in the nodes, links, and blobs picture, there will be no backtracking.

We have argued that backtracking is negligible close to the percolation threshold $p=p_c$ and in the dilute limit $p \ll p_c$. The simulations described in Sec. V support these conclusions, and, in addition, show that the effects of backtracking are small throughout the entire range of p values. Thus, Eq. (4.38) provides a good estimate of the time to failure for all values of p and N.

It remains for us to argue that the lengths of the critical and shortest paths are usually close to being equal. We must have $n(\Gamma_s,C) \le n(\Gamma_c,C)$. On the other hand, Eqs. (4.34) and (4.35) show that

$$n(\Gamma_c,C) \le n(\Gamma_s,C) + 2Q_0^{-1}[Q^-(\Gamma_c,C) - Q^-(\Gamma_s,C)] .$$

We now have the desired result:

$$n(\Gamma_s,C) \le n(\Gamma_c,C) \le n(\Gamma_s,C) + 2Q^-(\Gamma_c,C)/Q_0 .$$

We have argued that $\langle Q^-(\Gamma_c,C)\rangle$ is negligible. We therefore conclude that

$$\langle n(\Gamma_s,C)\rangle \cong \langle n(\Gamma_c,C)\rangle ,$$

as claimed.

E. Predictions of the shortest-path theory

Equation (4.38) relates the mean failure time to $\langle n(\Gamma_s,C)\rangle$, the average length of the shortest path that traverses the initial configuration of the network. Accordingly, we shall call the approximate theory that is obtained by neglecting backtracking across the critical path the "shortest-path theory."

Much is known about the behavior of $\langle n(\Gamma_s,C)\rangle$.[56] It has been proven that as the size of the network L tends to infinity,

$$\langle n(\Gamma_s,C)\rangle \sim \mu(p)L . \tag{4.39}$$

The first passage time constant $\mu(p)$ is positive for $p<p_c$ and is zero for $p>p_c$. As the percolation threshold p_c is approached from below, $\mu(p)$ tends to zero as $\mu(p) \sim (p_c-p)^\nu$. The exponent ν is exactly $\frac{4}{3}$ in two dimensions.[55] At the percolation threshold,

$$\langle n(\Gamma_s,C)\rangle \sim k \ln L \tag{4.40}$$

as $L \to \infty$. Here k is a constant. These predictions are consistent with scaling theory.[56]

Let us now consider the predictions of the shortest-path theory. For a given $p<p_c$, the mean failure time grows as $\langle T_f\rangle \sim \mu(p)t_0L$ as $L\to\infty$. The failure time tends to the constant $\mu(p)Q_0/j_0$ if the current density $j_0=I_0/L$ is held fixed as L grows large. If p is not greater than p_c but is close to it, we may use Eqs. (4.39) and (4.40) and the scaling hypothesis to yield

$$\langle T_f\rangle \sim \begin{cases} t_0 \ln L & \text{for } a \ll L \ll \xi , \\ (p_c-p)^{4/3}t_0L & \text{for } L \gg \xi . \end{cases} \tag{4.41}$$

Naturally, the failure time is zero for $p>p_c$.

An approach that is somewhat similar to our shortest-path theory has been developed in the theory of dielectric breakdown.[32–34,57] In their study of a continuum model for dielectric breakdown in metal-loaded dielectrics, Gyure and Beale assigned each path P that spanned the system from busbar to busbar a "gap" $x(P)$.[33,34] The value of $x(P)$ is equal to the length of the path that lies in the dielectric. Gyure and Beale noted that the path with the smallest gap tends to be close to the actual path that led to breakdown. Their Monte Carlo simulations also suggest that the breakdown field is approximately proportional to the minimum gap. Antecedents to the ideas of Gyure and Beale appear in Refs. 32 and 57.

V. SIMULATIONS OF FILMS WITH MULTIPLE CRACKS

In this section, we present the results of our simulations of electromigration in films with multiple cracks. We begin by demonstrating that the behavior of our model differs markedly from that of the random fuse network. We then test the Lifshitz-type and shortest-path theories developed in Sec. IV.

A. Comparison of the breakdown model of electromigration and the random fuse network

As we noted in Sec. II, our model of electromigration differs from the random fuse model because it is truly kinetic. In this section, we will show that our model differs from the random fuse model in three other important respects. In the random fuse network, the bond that carries the greater current (the so-called "hottest" bond) is always the next to fail. We shall show that in our model, the next bond to fail is usually not the hottest bond. In both the random fuse network and in our model, a critical path of broken bonds traverses the network once the network has failed. However, even if the initial configurations are the same in the two models, the critical paths are, in general, different. Finally, when the value of p is not small, the damage is much more widely distributed throughout the network in our model of electromigration than it is in the random fuse model.

We begin by comparing the breaking processes in the two models for a particularly simple initial configuration C_0. Suppose that at time $t=0$, there are three horizontal cracks, c_1, c_2, and c_3, in an $N_x \times N_y$ grid. The ith crack consists of ν_i adjacent broken vertical bonds for $i=1,2,3$. Further, suppose that cracks c_1 and c_2 are in the same row and that crack c_3 is in a different row than these two cracks (Fig. 7). Let the former row be denoted $R_{1,2}$ and let the latter be R_3. For simplicity, we consider the case in which $N_y \gg N_x$ and assume that the distance between rows $R_{1,2}$ and R_3 is much larger than the width of the network $N_x a$. With these assumptions, the current flow around the crack c_3 will be the same as if the other cracks were not present for $t<T_f$. Similarly, the current flow around the cracks c_1 and c_2 will be the same as if the crack c_3 were absent. Finally, we choose the ν_i's so that $\nu_3 > \nu_2 \geq \nu_1$ and $\nu_1+\nu_2>\nu_3$. Since ν_3 is greater than ν_1 and ν_2, the hottest bonds will be adjacent to the tips of crack c_3 at time $t=0$. (Actually, if the cracks c_1 and c_2 are very close together, the hottest bond could lie between them. We assume that this is not the case.)

Consider the breaking process that results from this initial configuration in the case of the random fuse model. The hottest bonds are the two vertical resistors adjacent to the ends of c_3. These bonds are therefore the first to fail. Once these bonds have failed, the hottest bonds are still at the tips of the crack c_3. Thus, the tips of this crack simply propagate laterally until they meet. The other two cracks (c_1 and c_2) do not grow at all, and the hottest bond is always the next to fail.

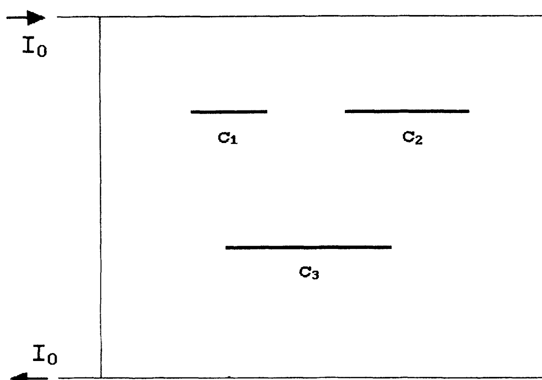

FIG. 7. The three cracks c_1, c_2, and c_3 present in the initial configuration C_0. The bonds dual to bonds that are insulating in the initial state are shown with solid lines.

Now consider the time evolution in the breakdown model of electromigration that ensues from the initial configuration C_0. Since the vertical distance between $R_{1,2}$ and R_3 is large, the currents in the vertical conducting bonds in these two rows are all directed downward. The special case in which $\nu_1=0$ was already discussed in Sec. IV B. Arguing in precisely the same way, we find that since $\nu_1+\nu_2>\nu_3$, the critical path is the horizontal line lying in row $R_{1,2}$. The crack c_3 does grow to some extent, because initially the hottest bonds are adjacent to its tips, and these bonds are the first to fail. However, the hottest bond is not always the next to fail—if it were, the crack c_3 would simply grow laterally until its tips met, and the critical path would lie in the row R_3.

To bring these conclusions into sharper focus, we performed simulations of the fuse model and the electromigration model in a 128×128 network. (Simulations with $N_y \gg N_x$ would be prohibitively time consuming.) In both models, we used the same initial configuration bearing three cracks. Cracks c_1 and c_2 were initially composed of seven broken vertical bonds, and were centered at the points (32,84.5) and (96,84.5), respectively. (We set $a=1$.) The third crack was centered at (64,42.5) and had $\nu_3=13$. In the case of the fuse model, only vertical bonds with height $y=42.5$ were broken during the simulation, and the critical path was a horizontal line containing the crack c_3. This is what we would expect on the basis of the preceding discussion. In contrast, the three cracks grew concurrently in the electromigration model. The number of broken bonds in the row $R_{1,2}$ grew more rapidly than the number of broken bonds in the row R_3, however (Fig. 8). After cracks 1 and 2 had fused to form a single crack, this crack grew still further, and ultimately its growth led to failure of the network as a whole. Of the 200 bonds that failed, only 85 were the hottest bond at the time they failed. Finally, although the critical crack was in row $R_{1,2}$, a total of 82 bonds were broken in row R_3 during the electromigration process.

Let us also compare the behavior of the random fuse model and our model of electromigration when the insulating bonds are initially randomly distributed. We generated a random initial configuration with $p=0.07$ for a 64×64 network, and then performed simulations of the failure process in the two models starting from this configuration. Figure 9 shows the final state in the random fuse network. Note that all of the broken bonds lie on the critical path. Figure 10 shows the final state in the breakdown model of electromigration. In this case, many bonds are broken that do not lie on the critical path, and there is extensive damage throughout the network. The critical path itself differs markedly from that found for the random fuse model, despite the fact that the initial

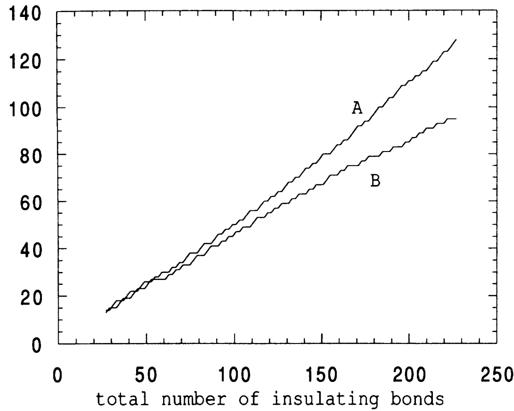

FIG. 8. The number of broken bonds in row $R_{1,2}$ (curve A) and R_3 (curve B) plotted vs the total number of insulating bonds.

configuration was the same in the two simulations. During the simulation of the electromigration model, each time we deduced which bond would break next, we recorded the current I_b passing through this bond before breaking it. We also recorded the current I_h passing through the hottest bond in the network at that time. Figure 11 shows the ratio I_b/I_h as a function of the total number of broken bonds. Initially, I_b/I_h was equal to one. However, at later times, the next bond to fail as usually not the hottest bond. There is an overall downward trend in the values of I_b/I_h, although even at the latest times it occasionally jumps up to 1. Of the 843 bonds that broke, only 11 were the hottest bonds at the time they failed. In contrast, the hottest bond is always the next to fail in the random fuse model, and I_b/I_h is always equal to 1.

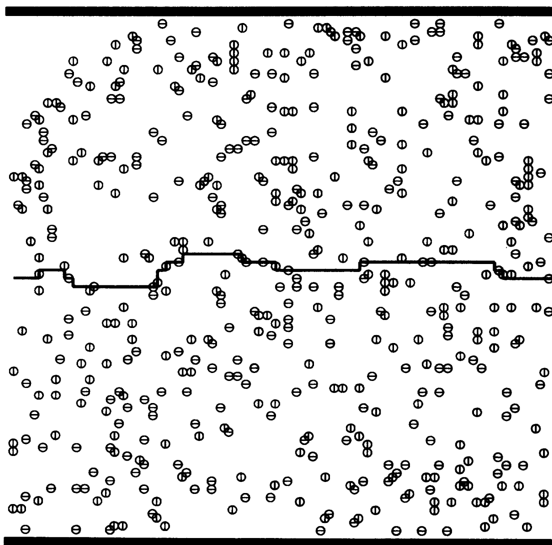

FIG. 9. The final and initial configurations of a 64×64 random fuse network with $p=0.07$. The bonds dual to bonds that are insulating in the final state are shown with solid lines. The critical path itself is shown with bold solid lines. Bonds that were insulating at time $t=0$ are circled, and the busbars are shown with thick solid bars at the top and bottom of the network.

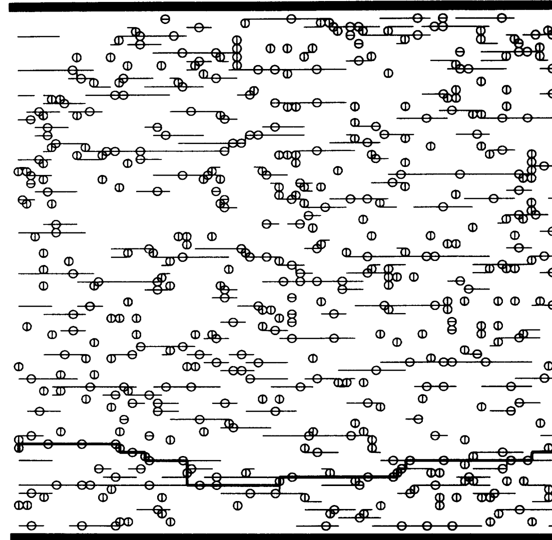

FIG. 10. The final and initial configurations of the breakdown model of electromigration for a 64×64 network with $p=0.07$. The initial configuration is the same as in Fig. 9. For the meaning of the various symbols, see the caption for Fig. 9.

B. Tests of the theories of the failure time

To test the approximate Lifshitz-type and shortest-path theories developed in Sec. IV, we performed simulations of our breakdown model of electromigration. Instead of solving Kirchhoff's equations directly, the Green's function formulation for the resistor network was solved using the conjugate gradient method.[52] This algorithm is an especially powerful means of finding for the current distribution in a resistor network, and is much more efficient than solving Kirchhoff's equations directly using the conjugate gradient method. The failure times were determined for a range of p values between 0

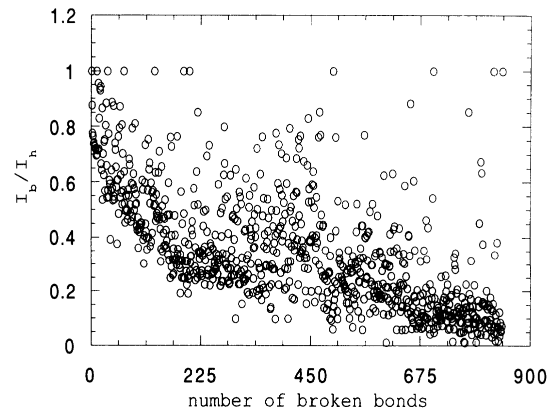

FIG. 11. I_b/I_h as a function of the total number of broken bonds for the same simulation as in Fig. 10.

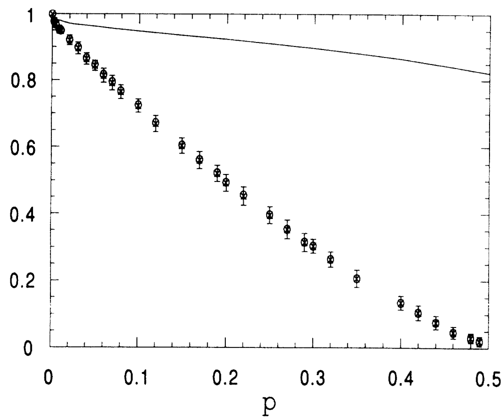

FIG. 12. The dimensionless failure time $(j_0 a/Q_0)\langle T_f\rangle$ (crosses with error bars), $\langle n(\Gamma_s,C)\rangle/N$ (open circles), and $1-\langle \nu_{\max}\rangle/N$ (solid curve) are plotted vs p for $0\leq p\leq 1/2$ for a 64×64 network.

and $p_c=\frac{1}{2}$. The grids studied had $N_x=N_y=N$ and $N=8$, 16, 32, and 64. For each value of p and N, an average over $\Omega(N)$ configurations was made. Ω was 5000 for $N=8$, 1000 for $N=16$, and 50 for both $N=32$ and 64. The current density $j_0=I_0/L$ and the charge Q_0 had the same values in all of the simulations.

To test the Lifshitz theory prediction,

$$\frac{j_0 a}{Q_0}\langle T_f\rangle \cong 1-\frac{\langle \nu_{\max}\rangle}{N} ,$$

we computed the value of $\nu_{\max}$ for a 64×64 network for a range of p values. For each value of p, an average over 10 000 configurations was made. Our results for the mean dimensionless failure time $(j_0 a/Q_0)\langle T_f\rangle$ and $1-\langle \nu_{\max}\rangle/N$ are plotted vs p in Figs. 12 and 13 for the 64×64 lattice. The Lifshitz theory is in reasonable agreement with the results of the simulations when p is small, but diverges widely from the $\langle T_f\rangle$ values obtained in the simulations for larger values of p.

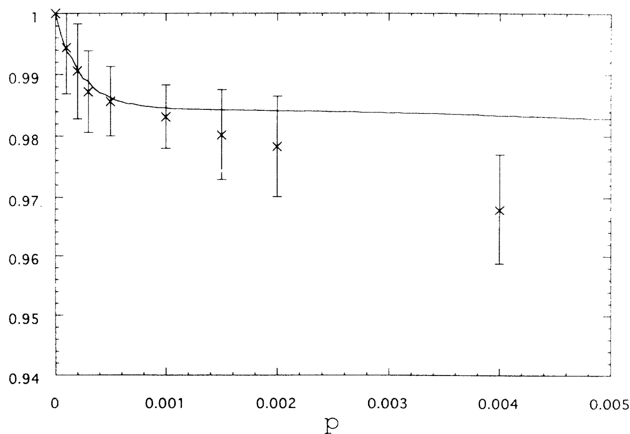

FIG. 13. The dimensionless failure time $(j_0 a/Q_0)\langle T_f\rangle$ (crosses with error bars), and $1-\langle \nu_{\max}\rangle/N$ (solid curve) are plotted vs p for $0\leq p\leq 0.005$ for a 64×64 network.

As we saw in Sec. IV D, two cracks are likely to coalesce to form a single crack only if they are in the same or adjacent rows. Thus, fusion and bridging are negligible if $pN\ll 1$. Since the possibility that these events occur is neglected in the Lifshitz-type theory, this theory should be a good approximation when $p\ll N^{-1}$, but not for larger values of p. This is in complete accord with the results shown in Figs. 12 and 13.

So that we could compare the simulation results with the predictions of the shortest-path theory, we computed the mean length of the shortest path $\langle n(\Gamma_s,C)\rangle$ that traversed the 64×64 network. The shortest-path lengths were calculated for the same set of initial configurations C as were used in our simulations of the electromigration process. These lengths were then averaged to yield an estimate of $\langle n(\Gamma_s,C)\rangle$. For a given configuration C, the length of the shortest path was determined using a straightforward modification of the "burning" algorithm.[53]

The computed values of $\langle n(\Gamma_s,C)\rangle/N$ are displayed in Fig. 12, along with the dimensionless failure time. The values of $(j_0 a/Q_0)\langle T_f\rangle$ and $\langle n(\Gamma_s,C)\rangle/N$ are virtually indistinguishable throughout the entire range of p values. Our results therefore provide strong support to our claim that Eq. (4.38) is a good approximation.

Although Eq. (4.38) is an excellent approximation, it is not exact. The relative error

$$R\equiv\frac{\langle n(\Gamma_s,C)\rangle t_0-\langle T_f\rangle}{\langle T_f\rangle}$$

we make in adopting Eq. (4.38) is not zero for $0<p<p_c$ and $N=64$ (Fig. 14). However, R never exceeds 0.7%, and is still smaller for p values close to 0 and p_c. All of our R values are nonnegative, and this is consistent with the inequality $\langle T_f\rangle\leq t_0\langle n(\Gamma_s,C)\rangle$ we obtained in Sec. IV B.

The shortest-path theory is a good approximation for $N=64$, but this is no guarantee that it remains a good approximation for larger values of N. In Fig. 15, we have plotted our results for R vs $1/\log_{10}N$ for $p=0.15$ and 0.4. For both values of p, the data can be fit to straight lines, yielding extrapolated values of R in the infinite size limit. For $p=0.15$, we find $R(N=\infty)=0.0074\pm 0.0005$, while

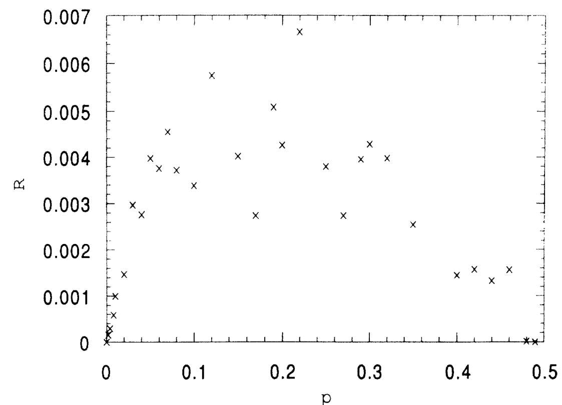

FIG. 14. The relative error R is plotted vs p for $N=64$.

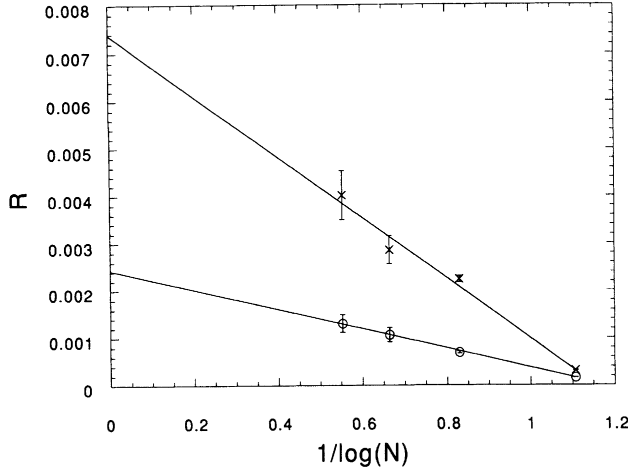

FIG. 15. R vs $1/\log_{10}N$ for $p=0.15$ (crosses with error bars) and 0.4 (open circles with error bars). The straight lines are least-squares fits to the data.

for $p=0.4$, we obtain $R(N=\infty)=0.0024\pm0.0002$. In both cases, the extrapolated relative errors are less than 1%. Thus, although R does increase with system size, it seems to asymptote to small values.

In Sec. IV D we argued that

$$\langle n(\Gamma_s,C)\rangle \cong \langle n(\Gamma_c,C)\rangle \ . \tag{5.1}$$

For the 64×64 network,

$$\langle n(\Gamma_c,C)-n(\Gamma_s,C)\rangle / \langle n(\Gamma_s,C)\rangle$$

was less than 0.032 for all values of p we studied, and was still smaller for p close to zero and p_c. For all of the values of p we examined, the length of the critical path was precisely equal to the length of the shortest path in more than half of the samples. Our simulations therefore are in good agreement with Eq. (5.1), and with the predictions of the shortest-path theory as a whole.

VI. FAILURE OF LONG CURRENT-CARRYING WIRES

So far, we have concentrated on the failure of square films. Unfortunately, experiments have not been performed yet with this type of geometry, and so the predictions made in Sec. IV E cannot be compared with experiment. All experiments done to date have been concerned with the lifetime of long, narrow wires. This is natural, since this is the issue of greatest practical importance in microelectronics. For this reason, in this section we will study the failure of long, narrow films with $L_y \gg L_x \gg a$.

The most complete experimental results on the lifetime of polycrystalline metal wires were obtained over two decades ago by Agarwala, Attardo, and Ingraham (AAI).[58] AAI used photolithography to make polycrystalline aluminum stripes of varying lengths L_y and widths L_x. The stripes were examined under a light microscope at a magnification of 500×, and were discarded if "macroscopic defects like notches" were observed. AAI determined the lifetime of each of the remaining stripes when subjected to a constant current I_0. All of the wires had the same thickness h and were subjected to the same constant current density $I_0/(L_x h)$.

AAI found that if L_y becomes large while L_x is held fixed,

$$\langle T_f\rangle \simeq \alpha(L_x)+\frac{\beta(L_x)}{L_y} \ , \tag{6.1}$$

where α and β are positive, increasing functions of L_x. They also observed that the variance of the distribution of T_f values decreased with the length of the wire L_y. In this section, we will use the shortest-path theory to account for the observations of AAI.

Consider the time to failure T_f of a rectangular network with fixed $p<p_c$ and $L_y \gg L_x \gg a$ that is subjected to a constant current density $j_0=I_0/L_x$. According to the shortest-path theory, $T_f \cong N_s t_0$, where N_s is the length of the shortest path that traverses the wire. We now partition the wire into $\nu=L_y/L_x$ square segments, each having sides of length L_x. Let $n_{s,i}$ be the length of the shortest path that traverses the ith segment, while remaining within the segment. Clearly, $N_s \le \min(n_{s,1},n_{s,2},\ldots,n_{s,\nu})$. In fact, since $L_x \gg a$, to an excellent approximation we have $N_s=\min(n_{s,1},n_{s,2},\ldots,n_{s,\nu})$. Let $P(n_s,L_x)$ be the probability that the length of the shortest path that traverses a square of side L_x is n_s, and let $F(n_s,L_x)=\sum_{k=0}^{n_s}P(k,L_x)$ be the corresponding cumulative distribution function. According to the asymptotic theory of extreme order statistics,[59]

$$\langle F(N_s,L_x)\rangle \cong \frac{1}{\nu} \tag{6.2}$$

for $\nu \gg 1$.

To determine the behavior of $\langle T_f\rangle$ for $\nu=L_y/L_x\gg1$, we need to know the form of the cumulative distribution function $F(n_s,L_x)$ when n_s is small. We are currently studying the distribution of shortest-path lengths, and we hope to determine the behavior of $\langle T_f\rangle$ for $L_y\gg L_x\gg a$. However, that work will not yield agreement with the experiments of AAI. This is because the values of $\langle N_s\rangle$ and $\langle T_f\rangle$ for the rectangular network tend to zero as $L_y\to\infty$. In contrast, AAI found that $\langle T_f\rangle$ tends to a nonzero constant as the length of the wire becomes large.

This apparent discrepancy between theory and experiment arises because samples with macroscopic notches were discarded by AAI. This screening removes the most severe defects, and leads to substantial changes in the asymptotic behavior of $\langle T_f\rangle$. The screening procedure employed in the experiments was rather subjective and was not described in detail. To estimate its effect, let us suppose that a sample was discarded if it had a crack of width w_c or greater in it. The threshold width w_c is a constant independent of both L_x and L_y, since all of the samples were examined with the same magnification. Suppose that a crack of width w was observed in a particular wire. The length of the shortest path traversing the wire (N_s) would then be approximately equal to $\lambda(L_x-w)$, where $\lambda<1$ is a constant of proportionality.

Thus, roughly speaking, a metal stripe would have been screened out if the length of the shortest path traversing it was less than a cutoff length $n_c \equiv \lambda(L_x - w_c)$.

As a result of this screening process, $P(n_s,L_x)$ is replaced by a new probability distribution $\tilde{P}(n_s,L_x)$ given by

$$\tilde{P}(n_s,L_x)=\begin{cases}\tilde{A}P(n_s,L_x) & \text{for } n_s \geq n_c \\ 0 & \text{for } n < n_c\ .\end{cases} \tag{6.3}$$

Here $\tilde{A}$ is a normalization constant; to be explicit, $\tilde{A}=[1-F(n_c,L_x)]^{-1}$. Let $\tilde{F}(n_s,L_x)$ be the new cumulative distribution function. Equation (6.2) is replaced by

$$\langle \tilde{F}(N_s,L_x)\rangle \cong \frac{1}{\nu}\ . \tag{6.4}$$

When n_s is close to n_c but is still greater than it, $\tilde{F}(n_s,L_x) \cong A(n_s-n_c)$, where $A=P(n_c,L_x)[1-F(n_c,L_x)]^{-1}$. Now when ν is large, in all likelihood N_s will be close to n_c. Thus, for $L_y \gg L_x$, Eq. (6.4) reduces to $A(\langle N_s\rangle - n_c) \cong 1/\nu$ or $\langle N_s\rangle \cong A^{-1}L_x/L_y + n_c$. Since $\langle T_f\rangle \cong \langle N_s\rangle t_0$, we have at last

$$\langle T_f\rangle \cong \frac{Q_0}{j_0}\left[\lambda\left[1-\frac{w_c}{L_x}\right]+\frac{A^{-1}}{L_y}\right] \tag{6.5}$$

for $L_y \gg L_x \gg a$.

Equation (6.5) is of precisely the form (6.1) found by AAI. In particular, the theory predicts that $\langle T_f\rangle$ asymptotes to a nonzero value as $L_y \to \infty$, and that the correction to the asymptotic value of $\langle T_f\rangle$ falls to zero as L_y^{-1}. Comparing Eqs. (6.1) and (6.5), we obtain

$$\alpha(L_x)=\frac{Q_0\lambda}{j_0}\left[1-\frac{w_c}{L_x}\right] \tag{6.6}$$

and

$$\beta(L_x)=\left[\frac{Q_0}{j_0}\right]\frac{1-F(n_c,L_x)}{P(n_c,L_x)}\ . \tag{6.7}$$

Thus, α and β are increasing functions of L_x, as observed by AAI.

As we have noted, AAI found that α is an increasing function of L_x. Actually, Agarwala, Attardo, and Ingraham went further and suggested that $\alpha(L_x) \propto L_x$. Unfortunately, there is too much scatter in their data to distinguish between this form for $\alpha(L_x)$ and ours, or to permit a detailed test of Eq. (6.6).

According to the asymptotic theory of extreme order statistics,[59] for $\nu \gg 1$

$$\text{var}[\tilde{F}(N_s,L_x)] \cong \frac{1}{\nu}\ , \tag{6.8}$$

where $\text{var}(x)$ denotes the variance of the random variable x. For $L_y \gg L_x$ this reduces to $\text{var}(N_s) \cong (A\nu)^{-1}$. Hence, for $L_y \gg L_x \gg a$,

$$\text{var}(T_f) \cong \left[\frac{Q_0}{j_0 A}\right]\frac{1}{L_y}\ . \tag{6.9}$$

Equation (6.9) shows that the width of the distribution of failure times decreases as the length of the wire grows large. This is again in agreement with the observations of AAI. The data of AAI have too much scatter to allow a detailed test of the predicted form of the decrease, however.

In sum, the shortest-path theory is able to satisfactorily account for the observations of AAI. It would be desirable to have further experiments done in the future in which the wires were not screened before life testing, however. Experiments of that kind would permit a more detailed comparison with the shortest-path theory. Improved tests of the theory would also become possible if the statistical errors in the experimental results were reduced by increasing the number of samples tested.

VII. CONCLUSIONS

In this paper, we introduced a kinetic breakdown model for the damage done to a polycrystalline metal thin film by electromigration. In our model, the metal film is represented by a regular grid of "wires." Initially, a fraction $1-p$ of these wires are conductors and the remainder are insulators. As current passes through a conductor, it is damaged by electromigration. A conducting wire fails irreversibly once a charge Q_0 has passed through it. Thus, wires that carry a heavy current load fail sooner than those that do not.

Our model was inspired by the random fuse model but is fundamentally different from it. The random fuse model is not a kinetic model, since failure occurs instantaneously when the applied voltage is sufficiently large. In contrast, our model is truly kinetic, since we can follow the breakdown process as a function of time. Our model was shown to differ from the random fuse model in several other important respects as well.

We began work on our model by studying the growth of a single crack oriented perpendicularly to the direction of the ambient current. As the crack length $2x$ grows large, the velocity of the crack tips v scales as $v(x) \sim x^{\alpha}$ in an infinite network. We argued that the value of the exponent α is exactly 2, and this result is in excellent agreement with our numerical work.

As a first attempt to construct a theory of the failure process when multiple cracks are present, we developed a Lifshitz-type theory for our model. We were encouraged to do so because the Lifshitz-type theory of Duxbury and co-workers[24–26] is quite successful in predicting the failure voltage of a random fuse network. Our Lifshitz-type theory is in good agreement with the results of our simulations of electromigration failure when $p \ll N^{-1}$, but for larger values of p, an entirely different approach is needed. This is because the interaction and fusion of cracks can only be ignored if the defects in the film are initially dilute.

We began our development of a theory of the failure process for arbitrary p by assigning a length $n(\Gamma)$ to closed self-avoiding paths Γ that wrap around the lattice once before closing. The failure time T_f is never greater than $n(\Gamma_s,C)t_0$, where $n(\Gamma_s,C)$ is the length of the shortest path that traverses the initial configuration C.

We then argued that, on average, the failure time T_f is in fact very close to being equal to $n(\Gamma_s,C)t_0$. We also argued that the length of the critical path $n(\Gamma_c,C)$ is almost always close to the length of the shortest path $n(\Gamma_s,C)$.

Our arguments were based to a large extent on a variational formulation of our problem that allowed us to construct upper and lower bounds on the time to failure. In the variational formulation, the critical path Γ_c for an initial configuration C minimizes a functional $F(\Gamma,C)$. If backtracking is neglected, this functional reduces to $Q_0 n(\Gamma,C)$. The critical path is just the shortest path in this approximation. We refer to this approximate theory as "the shortest-path theory."

Simulations of our model of electromigration damage are extremely time consuming, since Kirchhoff's equations for the network must be repeatedly solved. However, if we are content with knowing the approximate failure time, Kirchhoff's equations need never be solved: It is sufficient to compute the shortest-path length, and this can be done easily and with great speed. The shortest-path theory relates the time that a complex dynamical process comes to an end to a simple geometrical quantity, the length of the shortest path through the initial configuration.

Using the approximate shortest-path theory, we showed that the mean failure time of an $L\times L$ network tends to the constant $\mu(p)Q_0/j_0$ if the current density $j_0=I_0/L$ is held fixed as L grows large. This constant tends to zero as $(p_c-p)^{4/3}$ as the percolation threshold is approached.

We also used the shortest-path theory to account for the experimental results of Agarwala, Attardo, and Ingraham. AAI determined the lifetime of polycrystalline metal wires of varying lengths L_y and widths L_x when subjected to a constant current density. We argued that sample screening had an important effect on the experimental results. When this screening is taken into account, we find that the mean failure time and the width of the distribution of failure times depend on the length and width of the wire in a fashion consistent with the data of AAI. In particular, we found that $\langle T_f \rangle$ asymptotes to a nonzero value as $L_y\to\infty$, and that the correction to the asymptotic value of $\langle T_f \rangle$ falls to zero like L_y^{-1}.

In the future, we intend to study networks with more general forms of disorder than the simple percolative disorder employed here. However, we expect that results similar to those reported in this paper will still apply. We will also study the probability distribution of failure times, the lifetime of long unscreened wires, and the effects of Joule heating. Finally, we are currently investigating the possibility that variants of the shortest-path theory can be successfully applied to other models of breakdown in random media.

ACKNOWLEDGMENTS

We would like to thank P. D. Beale, B. J. Buchalter, F. M. d'Heurle, P. M. Duxbury, C. S. Galovich, M. P. Gelfand, and P. L. Leath for helpful discussions. This work was supported by NSF Grant No. DMR-9100257.

[1]H. B. Huntington, in *Diffusion in Solids—Recent Developments,* edited by A. S. Novick and J. J. Burton (Academic, New York, 1975).

[2]J. N. Pratt and R. G. R. Sellors, *Electrotransport in Metals and Alloys* (Trans Tech, Riehen, 1973).

[3]D. A. Rigney, in *Charge Transfer—Electronic Structure of Alloys,* edited by L. H. Bennett and R. H. Willens (AIME, New York, 1974).

[4]F. M. d'Heurle and P. S. Ho, in *Thin Films—Interdiffusion and Reactions,* edited by J. M. Poate, K. N. Tu, and J. W. Mayer (Wiley, New York, 1978).

[5]P. B. Ghate, Solid State Technol. **26**(3), 113 (1983).

[6]M. Ohring, J. Appl. Phys. **42**, 2653 (1971).

[7]R. Rosenberg and M. Ohring, J. Appl. Phys. **42**, 5671 (1971).

[8]J. R. Lloyd and S. Nakahara, Thin Solid Films **64**, 163 (1979).

[9]J. R. Lloyd and S. Nakahara, Thin Solid Films **72**, 451 (1980).

[10]H. L. Huang and J. S. Yang, J. Phys. D **20**, 493 (1987), and Refs. 1–5 therein.

[11]H. Suhl and P. A. Turner, J. Appl. Phys. **44**, 4891 (1973).

[12]K. P. Rodbell, M. V. Rodriguez, and P. J. Ficalora, J. Appl. Phys. **61**, 2844 (1987).

[13]A. Gangulee and F. M. d'Heurle, Thin Solid Films **25**, 317 (1975).

[14]J. M. Pierce and M. E. Thomas, Appl. Phys. Lett. **39**, 165 (1981).

[15]A. J. Patrinos, V. D. Vankar, and J. A. Schwarz, J. Appl. Phys. **63**, 5733 (1988).

[16]M. J. Attardo, R. Rutledge, and R. C. Jack, J. Appl. Phys. **42**, 4343 (1971).

[17]J. M. Schoen, J. Appl. Phys. **51**, 513 (1980).

[18]H. B. Huntington, A. Kalukin, P. P. Meng, Y. T. Shy, and S. Ahmad, J. Appl. Phys. **70**, 1359 (1991).

[19]R. A. Sigsbee, J. Appl. Phys. **44**, 2533 (1973).

[20]P. J. Marcoux, P. P. Merchant, V. Naroditsky, and W. D. Rehder, Hewlett-Packard J. **40**(6), 79 (1989).

[21]R. Kirchheim and U. Kaeber, J. Appl. Phys. **70**, 172 (1991).

[22]T. J. Smy, S. S. Winterton, and M. J. Brett, J. Appl. Phys. **73**, 2821 (1993).

[23]L. de Arcangelis, S. Redner, and H. J. Herrmann, J. Phys. (France) Lett. **46**, 585 (1985).

[24]P. M. Duxbury, P. D. Beale, and P. L. Leath, Phys. Rev. Lett. **57**, 1052 (1986).

[25]P. M. Duxbury, P. L. Leath, and P. D. Beale, Phys. Rev. B **36**, 367 (1987).

[26]P. M. Duxbury and P. L. Leath, J. Phys. A **20**, L411 (1987).

[27]M. Söderberg, Phys. Rev. B **35**, 352 (1987).

[28]H. Takayasu, Phys. Rev. Lett. **54**, 1099 (1985).

[29]B. K. Chakrabarti, K. K. Bardhan, and P. Ray, J. Phys. C **20**, L57 (1987).

[30]S. S. Manna and B. K. Chakrabarti, Phys. Rev. B **36**, 4078 (1987).

[31]P. D. Beale and P. M. Duxbury, Phys. Rev. B **37**, 2785 (1988).

[32]D. R. Bowman and D. Stroud, Phys. Rev. B **40**, 4641 (1989).

[33]M. F. Gyure and P. D. Beale, Phys. Rev. B **40**, 9533 (1989).

[34]M. F. Gyure and P. D. Beale, Phys. Rev. B **46**, 3736 (1992).

[35]R. M. Bradley, D. Kung, S. Doniach, and P. N. Strenski, J.

Phys. A **20**, L911 (1987).
[36]R. M. Bradley, D. Kung, P. N. Strenski, and S. Doniach, Physica B **152**, 282 (1988).
[37]P. L. Leath and W. Tang, Phys. Rev. B **39**, 6485 (1989).
[38]W. Xia and P. L. Leath, Phys. Rev. Lett. **63**, 1428 (1989).
[39]E. L. Hinrichsen, S. Roux, and A. Hansen, Physica C **167**, 433 (1990).
[40]P. Ray and B. K. Chakrabarti, Solid State Commun. **53**, 477 (1985).
[41]P. Ray and B. K. Chakrabarti, J. Phys. C **18**, L185 (1985).
[42]B. K. Chakrabarti, D. Chowdhury, and D. Stauffer, Z. Phys. B **62**, 344 (1986).
[43]M. Sahimi and J. D. Goddard, Phys. Rev. B **33**, 7848 (1986).
[44]P. D. Beale and D. J. Srolovitz, Phys. Rev. B **37**, 5500 (1988).
[45]A. Hansen, S. Roux, and H. J. Herrmann, J. Phys. (France) **50**, 733 (1989).
[46]G. N. Hassold and D. J. Srolovitz, Phys. Rev. B **39**, 9273 (1989).
[47]H. J. Herrmann, A. Hansen, and S. Roux, Phys. Rev. B **39**, 637 (1989).
[48]D. Sornette and C. Vanneste, Phys. Rev. Lett. **68**, 612 (1992).
[49]C. Vanneste and D. Sornette, J. Phys. (France) I **2**, 1621 (1992).
[50]A kinetic model of dielectric breakdown in a *homogeneous* medium was introduced in L. Niemeyer, L. Pietronero, and H. J. Wiesmann, Phys. Rev. Lett. **52**, 1033 (1984). The bond-breaking process itself was taken to be stochastic in the model of Niemeyer, Pietronero, and Wiesmann. In contrast, the disorder in our model comes from flaws present in the material at $t=0$.
[51]A brief account of some of the results described in this section has appeared in R. M. Bradley and K. Wu, J. Phys. A **26**, 327 (1994).
[52]K. Wu and R. M. Bradley, Phys. Rev. E **49**, 1712 (1994).
[53]H. J. Herrmann, D. C. Hong, and H. E. Stanley, J. Phys. A **17**, L261 (1984).
[54]Y. Kantor, J. Phys. A **19**, L497 (1986).
[55]D. Stauffer and A. Aharony, *Introduction to Percolation Theory* (Taylor and Francis, London, 1991).
[56]J. T. Chayes, L. Chayes, and R. Durrett, J. Stat. Phys. **45**, 933 (1986).
[57]R. B. Stinchcombe, P. M. Duxbury, and P. Shukla, J. Phys. A **19**, 3903 (1986).
[58]B. N. Agarwala, M. J. Attardo, and A. P. Ingraham, J. Appl. Phys. **41**, 3954 (1970).
[59]S. S. Wilks, *Mathematical Statistics* (Wiley, New York, 1962).